Theor Chim Acta (1996) 94: 345–381

Theoretica Chimica Acta

The electron correlation cusp

I. Overview and partial wave analysis of the Kais function

Harry F. King
Department of Chemistry, State University of New York, Buffalo, NY 14260, USA

Received May 22, 1996/Final revision received August 5, 1996, Accepted August 5, 1996

Abstract. The Kais function is an exact solution of the Schrödinger equation for a pair of electrons trapped in a parabolic potential well with r_{12}^{-1} electron–electron interaction. Partial wave analysis (PWA) of the Kais function yields $E_L = E + C_1(L + \bar{C}_2)^{-3} + O(L^{-5})$ where E is the exact energy and E_L the energy of a renormalized finite sum of partial waves omitting all waves with angular momentum $\ell > L$. Slight rearrangement of an earlier result by Hill shows that the corresponding full CI energy differs from E_L only by terms of order $O(L^{-5})$ with FCI values of C_1 and $\bar{C}_2$ identical to PWA values. The dimensionless $\bar{C}_2$ parameter is weakly dependent upon the size of the physical system. Its value is 0.788 for the Kais function, and 0.893 for the less diffuse helium atom, and approaches $\bar{C}_2 \to 1$ in the limit of an infinitely compact charge distribution. The ℓth energy increment satisfies an approximate virial theorem which becomes exact in the high ℓ limit. This analysis, formulated to facilitate use of the Maple system for symbolic computing, lays the mathematical ground work for subsequent studies of the electron correlation cusp problem. The direction of future papers in this series is outlined.

Key words: Correlation cusp – Partial wave analysis – Electron correlation – Hooke's law model – Configuration interaction convergence

1 Overview

This is the first in a series of papers on the electron correlation cusp, and this overview serves as an introduction to the entire series. We briefly review the theory of the correlation cusp problem, and propose a solution using perturbation theory. We also express our view of the unimportance of similar analytic features of the wave function associated with the coalescence of three or more charged particles.

The electrostatic potential energy function is infinite when two or more electrically charged particles coalesce. The nonrelativistic electronic Schrödinger equation is satisfied at that point by the singularity in the potential energy operator being somehow canceled by a kinetic energy operator. An infinite potential energy term, $V\psi$, can be canceled by an infinite kinetic energy term, $T\psi$, corresponding to the wave function having infinite curvature in some direction, i.e. a discontinuous

first derivative. An s-orbital exhibits such a cusp at the nucleus. The electron correlation cusp is the analogous discontinuity associated with the coalescence of two electrons [1, 2]. These analytic features of the wave function have been well appreciated since the earliest days of quantum theory. Hylleraas [3], Pluvinage [4], and Roothaan [5] stressed the importance of using basis functions that satisfy both cusp conditions for accurate variational calculations of the helium atom ground state wave function. In 1957 Kato [2] extended the analysis to a general, many-electron system and proved that at a point where two electrons coalesce away from a nucleus and away from all other electrons the first derivative of the wave function w.r.t. the interelectron separation, $r \equiv r_{12}$, averaged over a small sphere about the singularity at $r = 0$, is half the value of the wave function at that point:

$$\left\langle \left(\frac{\partial \Psi}{\partial r} \right)_{r=0} \right\rangle_{\text{average}} = \frac{1}{2} \Psi_{r=0}. \tag{1}$$

The theorem follows from the fact that the Hamiltonian is dominated at that point by just two terms: the potential energy operator, r_{12}^{-1}, and the kinetic energy operator for the motion of electron 1 relative to electron 2. Kato's analysis and nearly all subsequent studies of the electron correlation cusp [6–9] begin with a linear transformation of coordinates yielding relative and center-of-mass vectors and a set of complementary coordinates. The following position vectors differ from Kato's only by a scale factor.

$$\boldsymbol{r} = \boldsymbol{r}_1 - \boldsymbol{r}_2, \qquad r = |\boldsymbol{r}| = r_{12}, \tag{2}$$

$$\boldsymbol{R} = \tfrac{1}{2}(\boldsymbol{r}_1 + \boldsymbol{r}_2), \qquad R = |\boldsymbol{R}|. \tag{3}$$

The effect of spherical averaging is to remove the contribution of the $\ell = 1$ component of the wave function expanded in spherical harmonics whose arguments are the polar coordinates of the $\boldsymbol{r}$ vector. Averaging is unnecessary, of course, if the $\ell = 1$ component is zero. All odd-ℓ components vanish by exchange symmetry for a two-electron, singlet state, so the stronger form of (1) without spherical averaging then applies [10, 11]. Similarly, all even-ℓ components vanish for any wave function when two electrons come together with same spin. Then both lhs and rhs of (1) are zero corresponding to a Fermi hole. Otherwise one usually encounters a mixture of odd and even ℓ components [6, 9].

It is known that the variational energy error of a configuration interaction calculation, or of any other orbital-based method, is of order $O(L^{-3})$ or greater where L is the maximum orbital angular momentum in the finite orbital basis. This $O(L^{-3})$ limiting law is the most important practical consequence of the correlation cusp, and we will have much more to say about it later in this paper. We approach the $O(L^{-3})$ problem with the following hopes and expectations:

1. There exist modified Hamiltonians which lack the troublesome r_{12}^{-1} singularity and whose eigenfunctions are smooth, i.e. free of correlation cusps. Smoothing the cusps accelerates the rate of convergence of orbital-based expansion methods. It is desirable that these Hamiltonians have a simple first quantization representation, i.e. be defined in terms of differential operators and potential functions rather than their matrix representations.

2. There exist such modified Hamiltonians whose eigenfunctions differ significantly from those of the true Hamiltonian only locally, i.e. only in the immediate vicinity of the correlation cusp. Ideally the correction function falls off exponentially with increasing electron–electron separation.

3. These smooth wave functions can be computed to high accuracy using slightly modified, existing, orbital-based methods such as the MOLCAS program [12] or other multi-reference configuration interaction method with orbital-based, second-order, perturbation corrections (MRPT) [13–15].

4. Cusps in the wave function can be restored by a rapidly convergent Rayleigh–Schrödinger perturbation expansion with the reference problem defined by the modified Hamiltonian.

5. Energy errors introduced by removing correlation cusps can be adequately corrected in low-order perturbation theory. Hopefully first-order in the wave function and second-order in the energy will suffice for most applications.

6. The first-order variation–perturbation equations can be evaluated using exponentially short range, explicitly-correlated, geminals with explicit linear r_{12} dependence in the vicinity of the cusp. Here we refer to the perturbation expansion mentioned in items 4 and 5 and not that mentioned in item 3.

A traditional MRPT computation attempts to describe: (i) nondynamic electron correlation effects associated with nearly degenerate, partially filled orbitals; (ii) the correlation cusp, i.e. very short-range dynamic correlation effects; and (iii) longer-range dynamic correlation effects. In the proposed method the MRPT computation is still required for tasks (i) and (iii), which are the major tasks of any molecular electronic structure computation and tasks for which orbital-based methods are very well suited. The MRPT method is not, however, well suited to task (ii), and we would relieve it of that burden. The intent is not to reduce the computational effort of a traditional MRPT computation, but rather to approximately double the computational effort in the hope of achieving a significant increase in accuracy. The method is proposed for *ab initio* computations which aspire to sub-milli-Hartree accuracy for open-shell systems, as when computing a potential energy surface for a bond-breaking chemical reaction or other process which involves the making or breaking of electron pairs. The method could be applied to closed-shell systems, but then offers little advantage over simpler methods because correlation cusp errors tend to be invariant on a closed-shell potential energy surface.

Each of the six issues listed above raises questions to be addressed in this series of papers. Consider the first two items. How do we smooth out the singularities? What parameter measures extent of smoothness? Can we derive more general limiting laws, analogous to the $O(L^{-3})$ law, which describe how rate of convergence depends upon the value of the smoothing parameter? We begin to address these questions in the third paper of this series. The mathematical analysis is far from trivial. The literature on the $O(L^{-3})$ law is characterized by the mathematical virtuousity of the authors, so if we are to extend and generalize this theory then it is perhaps well to look for some way to simplify the analysis. That is the goal of the present paper.

The reader will note the emphasis here on analytic features of the wave function associated with the coalescence of two electrons with little regard for similar analytic features such as the nuclear cusp or the weak logarithmic singularities associated with the coalescence of three particles (either three electrons [16], or two electrons coming together at a nucleus [16–21]). This lack of concern is based on two more expectations, namely, that the nuclear cusp condition is important but easy to satisfy, while three-body conditions are difficult to satisfy but unimportant for energy calculations. Detailed behavior of the wave function when one or two electrons are near a nucleus is more important for some other applications as when

computing isotropic hyperfine coupling constants [22]. We do not propose to smooth nuclear cusps because they can be adequately described simply by including a few highly contracted s-type Gaussian functions in the orbital basis. Of the two classes of three-particle singularities, the electron–electron–nucleus case is probably the most important. It has been the subject of formal [3, 16–18, 20, 21, 24] and numerical analysis [19, 21, 25, 26], mainly in the context of highly accurate calculations for the helium atom. Two-particle cusp conditions can be satisfied exactly for the helium ground state using the Hylleraas S-state basis, $\psi_{k,\ell,m}$, expressed as a set of functions of r_1, r_2 and r_{12} or equivalently of the s, t, u variables [3],

$$s = r_2 + r_1, \tag{4}$$

$$t = r_2 - r_1, \tag{5}$$

$$u = r_{12}, \tag{6}$$

$$\psi_{k,\ell,m} = s^k t^\ell u^m e^{-s/2}, \tag{7}$$

where k, ℓ, m are nonnegative integers with ℓ an even integer for ^{1}S states. In 1935, Bartlett et al. [23] derived recurrence relations for the coefficients of the $\psi_{k,\ell,m}$ implied by the Schrödinger equation and showed that these equations have no solution. In other words, no expansion in Hylleraas functions provides a formal solution of the Schrödinger equation. Although the Hylleraas variational wave function exhibits incorrect analytic behavior when both electrons are near the origin, there is no fundamental limit to the precision of the variational energy. This follows from completeness of the $\psi_{k,\ell,m}$ basis established in 1977 by Klahn and Bingel [27]. While the importance of satisfying two-particle singularities for practical energy computations has been established beyond question, the practical importance of three-body singularities is debatable even for energy computations which aspire to extreme accuracy. The most accurate variational calculation reported to date of the nonrelativistic, clamped-nucleus, helium atom ground state energy is that of Freund et al. [21, 25] (FHM) whose basis includes the logarithmic terms introduced earlier by Frankowski [19] and for which convergence has been established [20]. On the other hand, Thakkar and Koga [28] (TK) recently obtained a variational upper bound that lies between the best 230-term and 475-term results of FHM. The TK basis has not been subjected to analysis as has the FHM basis, but it lacks logarithmic terms and clearly does not admit a formal solution of the Schrödinger equation. Nonetheless, the 308-term TK basis and the 475-term FHM basis yield variational energies that differ by only 4 femto-Hartrees. Thus the history of accurate variational computations for the helium atom repeats itself. In 1957 Kinoshita [24] first showed how to generate a formal solution by expanding in non-negative integral powers of the variables s, u/s and t/u, and used this basis set to compute the then-lowest helium atom variational energy, only to be displaced in the Guinness book of Records the following year by Pekeris [29], who used the original Hylleraas functions rearranged to computational advantage.

2 Introduction

Section 3 of this paper discusses a model system which is used extensively here and in subsequent papers to test our ideas. Particular attention is paid to a special case of the model for which the exact, ground state solution of the Schrödinger equation

is an elementary function. To the best of our knowledge, the existence of this particularly simple wave function was first pointed out in 1989 by Kais et al. [30], so we refer to it as the *Kais function*. Section 4 develops the mathematical techniques to be used in Section 5 to evaluate integrals over partial waves of the Kais function. Simple closed-form expressions for the partial waves are reported in Sect. 5.1. Expectation values of various operators acting on partial waves are evaluated in Sects. 5.2–5.5, Section 5.6 reports limiting laws expressed as asymptotic formulas for the energy error incurred when the partial wave expansion is truncated by omitting all waves with $\ell > L$. Section 5.7 supplies further details of the symbolic manipulations carried out using the Maple program [31].

In 1962, Schwartz [32] showed, by formal analysis of the first-order perturbation equation for the helium atom, that the basis set truncation energy error is $O(L^{-3})$, where L is the maximum angular momentum in a finite orbital basis. The $O(L^{-3})$ law was subsequently rederived and extended in various other formal analyses [11, 33] and verified numerically [34–36]. In 1985, Hill [11] derived the following asymptotic formula for the variational energy error of a two-electron, ^{1}S, full-CI, calculation assuming that the orbital basis is complete in subspaces with $\ell \leqslant L$ and making only a few highly plausible assumptions about the analytic form of the exact wave function:

$$\Delta E_L(FCI) = C_1(L+1)^{-3} + C_2 L^{-4} + O(L^{-5}). \tag{8}$$

Hill's analysis yields the C_1 and C_2 coefficients expressed as integrals over the exact wave function. Trivial manipulation of Eq. (8) yields Eq. (9) which is equivalent in the high-L limit and provides a better description of energy errors when L is small:

$$\Delta E_L = C_1(L+\bar{C}_2)^{-3} + O(L^{-5}). \tag{9}$$

These same Eqs. (8) and (9) emerge from an independent and completely rigorous partial wave analysis (PWA) of the Kais function. Values of the parameters C_1, C_2 and $\bar{C}_2$ depend upon the system being considered as shown in Table 10. The parameter values do not, however, depend upon the details of the analysis. The relationship between the wave function and PWA parameter values is precisely that derived by Hill and given in Eqs. (47)–(50) below. The interacting electrons are trapped in a Coulomb well in Hill's analysis, and in a parabolic well in our partial wave analysis. The wave function is determined by the Ritz method in Hill's analysis and by generalized Fourier expansion in our analysis. In other words, Hill varies the wave function within a given subspace to minimize the energy. We project the exact wave function onto the subspace. None of these differences are important. That these details of the analysis affect only the unspecified terms of order $O(L^{-5})$ in Eqs. (8) and (9) testifies to the fact that the $O(L^{-3})$ limiting law is entirely a consequence of the linear dependence of the wave function upon interelectron separation when electrons are close together. This linear dependence, which is itself a consequence of the singularity in the electron–electron interaction, is the motivation for early [3] and more modern [37] methods for introducing explicit r_{ij} dependence into variational wave functions.

3 Hooke's law model

Because electron repulsion and kinetic energy operators dominate the Hamiltonian in the vicinity of the correlation cusp, one retains the essential physics when the remaining one-electron operators are replaced by parabolic potentials. The

relatively unimportant one-electron operators create major problems for the study of the correlation cusp in real atoms and molecules, so this constitutes an enormous simplification leading to the so-called Hooke's law model (HLM). The Hamiltonian for two interacting electrons trapped in a parabolic potential well with spring constant k is given in Eqs. (10)–(12). (We adopt atomic units, $e = m_e = \hbar = 1$, and denote the Hartree and micro-Hartree atomic units of energy by H and μH, respectively.)

$$\mathscr{H}(1, 2) = h(1) + h(2) + g(r_{12}), \tag{10}$$

$$h(i) = -\tfrac{1}{2}\nabla_i^2 + \tfrac{1}{2}kr_i^2, \tag{11}$$

$$g(r) = r^{-1}. \tag{12}$$

The two-electron HLM first appeared in the quantum chemistry literature in a 1962 paper by Kestner and Sinanoğlu [38], although it had been employed even earlier in nuclear physics. The model was subsequently used to illustrate various concepts and methods in perturbation theory [39], in the theory of highly excited electronic states [40], dimensional scaling theory [30], and density functional theory [41–43]. The three-electron HLM was used by White and Stillinger [16] to study three-particle logarithmic singularities mentioned in Sect. 1 above. The coordinate[5] transformation (Eqs. (2), (3)) completely separates the 6-D Schrödinger equation leading to a pair of uncoupled central field problems [44]. Note, for future reference, that this is true for any $g(r)$.

$$r_1^2 + r_2^2 = 2R^2 + \tfrac{1}{2}r^2, \tag{13}$$

$$\mathscr{H}(1, 2) = \mathscr{H}_R + \mathscr{H}_r, \tag{14}$$

$$E = E_R + E_r, \tag{15}$$

$$\mathscr{H}_R = -\tfrac{1}{4}\nabla_R^2 + kR^2, \tag{16}$$

$$\mathscr{H}_r = -\nabla_r^2 + \tfrac{1}{4}k^2r^2 + g(r), \tag{17}$$

$$\Psi(1, 2) = \Psi(\boldsymbol{R})\psi(r), \tag{18}$$

$$\Psi(\boldsymbol{R}) = F(R)\,Y_{LM}(\Theta, \Phi), \tag{19}$$

$$\psi(\boldsymbol{r}) = f(r)\,Y_{\ell m}(\theta, \phi). \tag{20}$$

Here $\Psi(1, 2)$, $\Psi(\boldsymbol{R})$ and $\psi(\boldsymbol{r})$ are normalized eigenfunctions of $\mathscr{H}(1, 2)$, $\mathscr{H}_R$ and $\mathscr{H}_r$ with eigenvalues E, E_R and E_r, respectively. Equation (13) exhibits the simplifying feature of the Hooke's law model, namely, that the one-electron potential is separable in the transformed coordinate system as well as in the original single-particle coordinates. We refer to $\Psi(\boldsymbol{R})$ and $\psi(\boldsymbol{r})$ as the external and internal wave functions, respectively, reminiscent of Eddington's extracule and intracule [45]. Similarly, (L, M) and (ℓ, m) are the respective external and internal angular momentum quantum numbers [46]. The even ℓ states are singlets and the odd ℓ states are triplets. Note that the kinetic energy operators in Eqs. (16) and (17) reflect the fact that the external (total) and internal (reduced) masses of the electron pair are 2 and 1/2 atomic units, respectively.

The external radial factor, $F(R)$ is that of the familiar three-dimensional harmonic oscillator, i.e. a product of a Gaussian and a polynomial. The internal radial factor can be expressed as the product of a Gaussian and a power series:

$$f(r) = Nr^{\ell}\left(1 + \frac{r}{2\ell + 2} + \cdots\right)\exp\left(\frac{-\sqrt{k}r^2}{4}\right). \tag{21}$$

Taut [44] gives the recurrence relation for the additional terms in the series and shows that the series terminates in special cases, i.e. for particular stationary states and particular values of k and ℓ. The simplest of these special cases is that with $\ell = 0$, $k = 1/4$, $E_r = 5/4$, discovered previously by Kais and co-workers [30, 41]. This, the Kais function, corresponds to an electron density roughly equal to that of the hydride ion. (See discussion below.) All other special cases have smaller k values, and thus lower electron densities, which makes them less representative of typical atomic and molecular systems, although they do find use in other areas of physics [43]. The leading terms shown explicitly in Eq. (21) dominate the behavior of $f(r)$ in the electron correlation cusp region. Note that these two terms are independent of the value of the spring constant k, and depend only on ℓ, independent of the other five quantum numbers for this model. As expected, an $\ell = 0$ state of the HLM satisfies (1) without spherical averaging. Higher ℓ states illustrate more general cusp conditions treated in detail by Kutzelnigg and Morgan [8] and Rassolov and Chipman [9]. The Kais function is the ground state wave function for spring constant $k = 1/4$ atomic units. Before undertaking a detailed analysis of the ground state, let us briefly survey the low lying electronic states of the model.

Using atom-like notation, let the three-dimensional harmonic oscillator orbitals be denoted $1s$, $2p$, $3s$, $3d$, etc. Note that the harmonic oscillator lacks the $2s$ and $3p$ orbitals. A three-dimensional oscillator with force constant k has the same mean squared $1s$ orbital radius as does the hydrogen-like atom with effective atomic number Z_{eff} when these parameters are related as follows:

$$Z_{\text{eff}} = \sqrt{2}\,k^{1/4} \quad \text{same } \langle r^2 \rangle_{1s}. \tag{22}$$

Alternately, one can equate $1s \rightarrow 2p$ excitation energies.

$$Z_{\text{eff}} = \sqrt{8/3}\,k^{1/4} \quad \text{same } \Delta E_{1s-2p}. \tag{23}$$

By either criterion one concludes that the Kais function corresponds roughly to the hydride ion ground state. An HLM with spring constant in the range $k = 2.3 \rightarrow 4.0$ would be a better model of the helium atom, but none of the special cases discussed by Taut [44] fall in this range. The lowest ten electronic states for $k = 1/4$ are described in Table 1 and Figs. 1 and 2. Only the lowest E_r for $k = 1/4$ is known exactly, but highly accurate values of all others can be computed by numerical solution of a one-dimensional differential eigenvalue equation using the so-called shooting method [47]. Note that these ten states include examples of purely dynamic electron correlation, e.g. the ^1S_g ground state, and examples of non-dynamic correlation, e.g. the ^1D_g states. The evenly spaced energy levels, labeled E^o in Table 1 and Fig. 1, are those for a pair of non-interacting electrons, i.e. they are simple sums of orbital energies. Electron–electron repulsion raises the ^1S_g ground state energy by exactly 0.5 H, comparable to the value 0.47225 H for the hydride ion. The 3.82 eV singlet–triplet splitting of the first excited state, shown on the right side of Fig. 1, is directly related to the different internal radial functions, $f(r)$, plotted in Fig. 2. Because the orbital angular momentum in the lowest ^1P state is purely external, it has the same $f(r)$ factor as does the ground state, and the effect of electron–electron interaction is to raise the ^1P energy also by 0.5 H. By contrast, the orbital angular momentum in the lowest ^3P state is internal, and its $f(r)$ factor has a node at the origin resulting in reduced electron repulsion energy. This is, of course, the story of the Fermi hole told in every quantum chemistry text book, but unlike the usual text book discussion, this version of the story draws attention to

Table 1. The ten lowest-lying electronic states of the two-electron Hooke's law model with spring constant $k = \frac{1}{4}$ atomic units. Energies are reported in Hartrees. Listed in column 4 is the state energy, E^0, for noninteracting electrons, $g(r) = 0$. All other quantities are computed using $g(r) = 1/r$. The last column gives the label of the appropriate internal radial function plotted in Fig. 2

Level	Term Symbol	E	E^0	Dominant Configurations	External		Internal		
					E_R	L	E_r	ℓ	$f(r)$
1	^1S_g	2.0000000000	1.5	$1s^2$	0.75	0	1.2500000000	0	s
2	^3P_u	2.3596570599	2.0	$1s\,2p$	0.75	0	1.6096570599	1	p
3	^1P_u	2.5000000000	2.0	$1s\,2p$	1.25	1	1.2500000000	0	s
4	^1D_g	2.7936138979	2.5	$1s\,3d$, $2p^2$	0.75	0	2.0436138979	2	d
5	^3S_g	2.8596570599	2.5	$1s\,3s$	1.25	1	1.6096570599	1	p
6	^3P_g	2.8596570599	2.5	$2p^2$	1.25	1	1.6096570599	1	p
7	^3D_g	2.8596570599	2.5	$1s\,3d$	1.25	1	1.6096570599	1	p
8	^1S_g	2.9401169182	2.5	$1s\,3s$, $2p^2$	0.75	0	2.1901169182	0	s^*
9	^1S_g	3.0000000000	2.5	$1s\,3s$, $2p^2$	1.75	0	1.2500000000	0	s
10	^1D_g	3.0000000000	2.5	$1s\,3d$, $2p^2$	1.75	2	1.2500000000	0	s

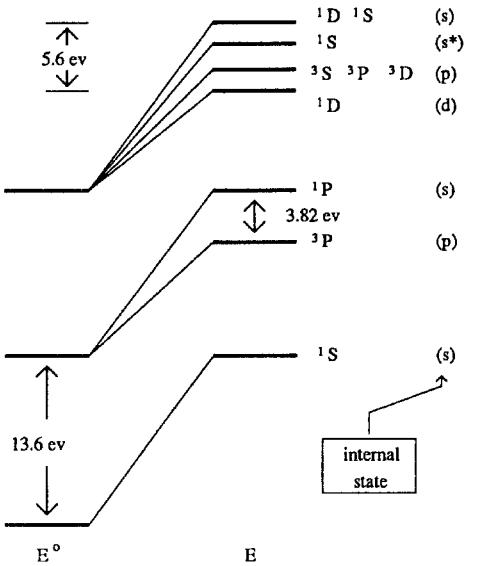

Fig. 1. Energy levels of the two-electron Hooke's law model with $k = 1/4$. Energy levels on the left, E^0, are those for noninteracting electrons

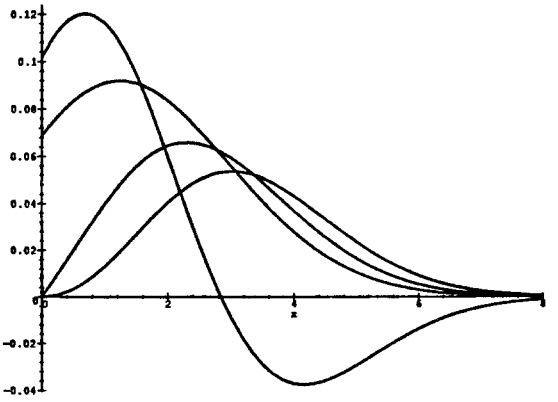

Fig. 2. Radial factors, $f(r)$, for the internal state wave function for the two-electron Hooke's law model with $k = 1/4$. The horizontal axis is the inter-electron separation, r, and extends to 8 Bohr. The states from top to bottom at left side of the figure are: s^*, s, p, and d. The order is reversed on the right side of the figure

the role of internal orbital angular momentum and to the fact that centrifugal force plays a role in reducing electron repulsion energy. For a similar discussion with somewhat different emphasis the reader is referred to a paper by Kutzelnigg and Morgan [8].

The Pauli exclusion principle requires that ℓ be odd (and thus nonzero) in triplet states, so the centrifugal force effect and Fermi holes are both intimately associated with triplet states. For singlets the Pauli exclusion principle requires that ℓ be even but not necessarily zero. Consider the two ^1D_g states shown in Fig. 1. These states are degenerate in the absence of electron–electron interaction, but are separated by 5.6 eV when the interaction is introduced. This is not, of course, a singlet–triplet splitting, but it is an analogous example of the effect of internal versus external orbital angular momentum. The orbital angular momentum of the lower ^1D_g state is entirely internal, while that of the upper ^1D_g state is entirely

external. Again the low-r behavior of the relevant $f(r)$ factors is associated with the differences in electron repulsion energies. From inspection of either Eq. (21) or Fig. 2 one correctly predicts that the lower ^1D_g state should lie below the three triplet states all having the same E^o values, in violation of Hund's rules. In a very recent reexamination of Hund's rules, Kutzelnigg and Morgan [48] point out that such violations are characteristic of nearly degenerate sd and p^2 configurations because resonant interaction stabilizes the $(sd)\,^1D$ state but not the $(sd)\,^3D$ state, since there exists no comparable $(p^2)\,^3D$ component with which to interact. They point out that such a violation of Hund's rules is observed in the atomic spectrum of neutral magnesium [49]. Note in Table 1 that level 4, ^1D, lies 1.80 eV below level 7, ^3D. This can be compared with the $(3s\,3d)\,^1D$ state of the magnesium atom which lies 0.193 eV below $(3s\,3d)\,^3D$. That the magnitude of the effect is smaller in the atom can be attributed reasonably to there being a strict degeneracy in the model but only a near degeneracy in the atom. Note that L and ℓ are good quantum numbers for the model, but that mixing occurs in real atoms and molecules. The above discussion leads us to predict that an appropriate analysis of the lowest ^1D state of the magnesium atom would show that an unusually large fraction of its orbital angular momentum is internal (associated with rotation of an electron pair about their instantaneous center of mass rather than about the nucleus) and that this spinning motion tends to keep them apart and so reduce their electrostatic interaction energy.

The remainder of this paper is concerned exclusively with the ground state of the two-electron HLM with $k = 1/4$ for which the exact, normalized, nonrelativistic wave function is the Kais function, $\Psi(1, 2)$:

$$\Psi(1, 2) = \Psi(R)\psi(r) = N(1 + r_{12}/2)\exp(-(r_1^2 + r_2^2)/4), \tag{24}$$

$$\Psi(R) = \pi^{-3/4}\exp(-R^2/2), \tag{25}$$

$$\psi(r) = \pi^{3/4} N(1 + r/2)\exp(-r^2/8), \tag{26}$$

$$E_R = \tfrac{3}{4}, \tag{27}$$

$$E_r = \tfrac{5}{4}, \tag{28}$$

$$4\pi\int_0^\infty \Psi(R)^2 R^2\,dR = 1, \tag{29}$$

$$4\pi\int_0^\infty \Psi(r)^2 r^2\,dr = 1, \tag{30}$$

$$N = (2\pi)^{-1}(5\pi + 8\sqrt{\pi})^{-1/2}. \tag{31}$$

Let $\Psi^o(1, 2)$ denote the corresponding $k = 1/4$ ground state wave function for non-interacting electrons.

$$\Psi^o(1, 2) = \Psi(R)\psi^o(r) = (2\pi)^{-3/4}\exp(-(r_1^2 + r_2^2)/4), \tag{32}$$

$$\psi^o(r) = (4\pi)^{-3/2}\exp(-r^2/8), \tag{33}$$

$$E_r^o = 3/4. \tag{34}$$

Averages taken over $\Psi^o(1, 2)$ or $\Psi(1, 2)$ are denoted by $\langle\,\rangle^o$ or $\langle\,\rangle$, respectively. For example, $\langle T\rangle^o$ and $\langle T\rangle$ are expectation values of the kinetic energy before and after the wave function has relaxed in the field of electron–electron interaction. One might have thought that relaxation, i.e. cusp formation, would decrease the

potential energy and increase the kinetic energy, but inspection of (39), (40), (43) and (44) shows that cusp formation is accompanied by an overall expansion of the wave function with the net result being a 2.33 eV reduction in kinetic energy and a 0.58 eV increase in potential energy:

$$\langle R^2 \rangle = \langle R^2 \rangle^\circ = 3/2, \tag{35}$$

$$\langle r_{12}^2 \rangle = 4\pi \int_0^\infty r^4 \psi(r)^2 \, dr \tag{36}$$

$$= \frac{42\sqrt{\pi} + 64}{5\sqrt{\pi} + 8} = 8.2102272030, \tag{37}$$

$$\langle r_{12}^2 \rangle^\circ = 6, \tag{38}$$

$$\langle r_1^2 \rangle = \frac{18\sqrt{\pi} + 28}{5\sqrt{\pi} + 8} = 3.5525568007, \tag{39}$$

$$\langle r_1^2 \rangle^\circ = 3, \tag{40}$$

$$\langle r_{12}^{-1} \rangle = \frac{2\sqrt{\pi} + 4}{5\sqrt{\pi} + 8} = 0.4474431992, \tag{41}$$

$$\langle r_{12}^{-1} \rangle^\circ = 1/\sqrt{\pi} = 0.5641895835, \tag{42}$$

$$\langle T \rangle = \frac{7\sqrt{\pi} + 10}{10\sqrt{\pi} + 16} = 0.6644176006, \tag{43}$$

$$\langle T \rangle^\circ = \tfrac{3}{4}. \tag{44}$$

$$E = 2 \tag{45}$$

The radial distribution function for the Kais function has been reported earlier [41]. We adopt the normalization $\int p(r)\,dr = 1$.

$$p(r_1) = \frac{4}{(5\pi + 8\sqrt{\pi})} \times \left[r_1^2 \exp(-r_1^2) + \frac{\sqrt{2\pi}}{8} \exp(-r_1^2/2)[7r_1^2 + r_1^4 + 4(r_1 + r_1^3)\,\mathrm{erf}\,(r_1/\sqrt{2})] \right]. \tag{46}$$

Finally, we evaluate the two integrals introduced by Hill [11,50] whose values are required in Sects. 5.6 and 5.7 below. Let $\Psi(1, 1)$ denote the value of the wave function when both electrons are at the same position, $\boldsymbol{r}_2 = \boldsymbol{r}_1$.

$$C_1 = 2\pi^2 \int_0^\infty r_1^5 \, \Psi^2(1, 1)\, dr_1 \tag{47}$$

$$= \frac{1}{10\pi + 16\sqrt{\pi}} = 0.01672934927, \tag{48}$$

$$C_2 = \frac{12\pi}{5} \int_0^\infty r_1^6 \, \Psi^2(1, 1)\, dr_1 \tag{49}$$

$$= \frac{9}{16\pi(5\sqrt{\pi} + 8)} = 0.01061834017. \tag{50}$$

4 Mathematical preliminaries

In Sect. 4.1 we define an infinite class of two-dimensional integrals designated as having *standard form*. The class is partitioned into six *types* each with a designated *representative* from which all other integrals of that type can be evaluated by recurrence. These same recurrence relations are used to derive numerically stable continued fraction formulas for the evaluation of integrals with large index values. The integration formulas derived here play a key role in the partial wave analysis in Sect. 5. For example, the $O(L^{-3})$ limiting law mentioned in the Introduction to this paper is eventually derived from asymptotic formulas obtained from the large-index formulas derived here. Section 4.2 develops another useful continued fraction formula, for integrals over products of three Legendre polynomials, that is encountered when evaluating electron repulsion integrals.

4.1 Integrals with standard form

The $M(p, q)$ integral defined in (51) whose indices are integers such that $p \geqslant 0$ and $p + q \geqslant -1$ is said to be in standard form:

$$M(p, q) \equiv \int_0^\infty \mathrm{e}^{-x^2/2} x^p \, \mathrm{d}x \int_{y=x}^{y=\infty} e^{-y^2/2} y^q \, \mathrm{d}y. \tag{51}$$

All such integrals converge. Integration by parts over x or y in (51) leads to a recurrence relation for the p or q index, respectively,

$$M(p, q) = (p-1) M(p-2, q) - \frac{1}{2} \Gamma\left(\frac{p+q}{2}\right), \tag{52}$$

$$M(p, q) = (q-1) M(p, q-2) + \frac{1}{2} \Gamma\left(\frac{p+q}{2}\right). \tag{53}$$

Figure 3 shows how the various $M(p, q)$ integrals are related by these recurrence relations. Each integral is related by (52) to the integrals lying two steps above or below it in the figure. Similarly, an $M(p, q)$ integral is related by (53) to the integrals two steps to the left or to the right in Fig. 3, except that odd-negative q's are not so related to odd-positive q's. Integrals related by a recurrence relation are said to be of the same type. There are six types labeled (a–f) in Fig. 3. Each type is represented by the member with minimal p and $|q|$ indices. Values of the six representatives are listed below:

$$M(0, -1) = \chi, \tag{54}$$

$$M(0, 0) = \tfrac{1}{4}\pi, \tag{55}$$

$$M(0, 1) = \tfrac{1}{2}\sqrt{\pi}, \tag{56}$$

$$M(1, -1) = \ln(\sqrt{2}), \tag{57}$$

$$M(1, 0) = \tfrac{1}{2}(\sqrt{2} - 1)\sqrt{\pi}, \tag{58}$$

$$M(1, 1) = \tfrac{1}{2}. \tag{59}$$

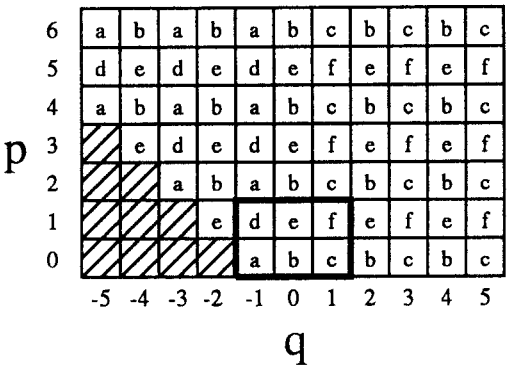

Fig. 3. The six types of $M(p, q)$ integrals. Two integrals are said to be of the same type if they are related by recurrence relations. The six representatives are enclosed in the small rectangle at the bottom center of the figure

The constant χ in (54) is the value of the following definite integral which has been evaluated numerically. We refer to it as the Kais constant:

$$\chi \equiv \sqrt{\pi/2}\int_0^\infty x^{-1}\,\mathrm{erf}\,(x)\,e^{-x^2}\,dx \tag{60}$$

$$= 1.10463797686806655691643 54. \tag{61}$$

All $M(p, q)$ integrals with indices in the shaded region of Fig. 3 are infinite. All others are finite and can be evaluated starting with the known representative value and repeatedly applying Eqs. (52) and (53). All type-a integrals, for example, have the form $\alpha\chi + \beta\sqrt{\pi}$ where α and β are rational numbers (ratios of integers). The $\alpha\chi$ term originates with the a-type representative value (54). The $\beta\sqrt{\pi}$ term is generated by gamma functions with half-integer arguments

$$\Gamma\left(n + \frac{1}{2}\right) = \frac{(2n)!\sqrt{\pi}}{n!\,4^n} \quad \text{integer } n. \tag{62}$$

For very large p and q indices it is useful to have an alternative method. Consider an alternative labeling scheme with three indices:

$$\bar{M}(p, q; \ell) \equiv M(2\ell + p,\ -2\ell + q). \tag{63}$$

This proves to be a useful but not a unique notation, for example,

$$\bar{M}(6,\ -1; \ell) = \bar{M}(4, 1; \ell + 1) = \bar{M}(2, 3; \ell + 2). \tag{64}$$

Integrals $\bar{M}(p, q; \ell)$ and $M(p, q)$ are said to be of the same type since they are both related by recurrence relations to the same representative. In particular, $\bar{M}(p, q; \ell)$ and $\bar{M}(p, q; \ell + 1)$ are of the same type and are directly related by (65):

$$(2\ell + 1 - q)\,\bar{M}(p, q; \ell + 1) + (2\ell + 1 + p)\,\bar{M}(p, q; \ell) = \Gamma\left((p + q + 2)/2\right) \tag{65}$$

Inspection of (51) shows that the integrand of $\bar{M}(p, q; \ell + 1)$ is everywhere less than or equal to that of $\bar{M}(p, q; \ell)$, thus

$$\bar{M}(p, q; \ell + 1) < \bar{M}(p, q; \ell) \tag{66}$$

Equations (65) and (66) establish the following bounds:

$$\frac{\Gamma((p + q + 2)/2)}{4\ell + 2 + p - q} < \bar{M}(p, q; \ell) < \frac{\Gamma(p + q + 2)/2)}{4\ell - 2 + p - q}. \tag{67}$$

So a sequence of $\bar{M}(p, q; \ell)$ with fixed p and q decreases monotonically with increasing ℓ approximately as ℓ^{-1}. This suggests that we look for continued fraction formulas with ℓ in the denominators. When each of the two $\bar{M}$ factors in (65) is replaced by a continued fraction formula with unknown parameters, one obtains an infinite system of equations which can be solved for the values of the unknown parameters. When $p = q = 0$ the resulting formula is

$$\bar{M}(0, 0; \ell) = 1/a_1, \tag{68}$$

$$a_k = 4\ell + (2k)^2/a_{k+1}. \tag{69}$$

Let this continued fraction expression be terminated by setting $a_k = 4\ell$ when $k = k_{\max}$, where the value of $k_{\max}$ is arbitrary. It can be shown that Eq. (68) then provides an upper or lower bound on $\bar{M}(0, 0; \ell)$ when $k_{\max}$ is odd or even, respectively. This procedure is numerically stable (completely free of differencing errors), and unlike an asymptotic expansion, converges absolutely w.r.t. increasing $k_{\max}$ for all $\ell > 0$. When $\ell > 9$ and $k_{\max} > 9$ the terminated continued fraction procedure gives $\bar{M}(0, 0; \ell)$ to at least 15 significant figures. The terminated continued fraction (perhaps, it should be called a discontinued fraction) can be rearranged into the form of a Padé approximation,

$$\bar{M}(0, 0; \ell) \approx P_{\text{num}}(\ell)/P_{\text{denom}}(\ell), \tag{70}$$

where P_{num} and P_{denom} are polynomials in ℓ of degree $k_{\max} - 1$ and $k_{\max}$, respectively, whose coefficients are positive integers. Similarly, one obtains continued fraction formulas for a-type integrals:

$$\bar{M}(2n, -1; \ell) = \Gamma(n + \tfrac{1}{2})/a_1, \tag{71}$$

$$a_k = 4\ell + 2n + 1 + 2k(2k + 2n - 1)/a_{k+1}. \tag{72}$$

To test our Maple programs, we evaluated various $\bar{M}(p, q; \ell)$ using continued fraction formulas with large ℓ and $k_{\max}$ and compared the results with numerical values obtained using Eqs. (52)–(60) with χ evaluated to higher accuracy than reported in Eq. (61). Agreement to 60 significant figures was achieved rather easily. Note that Eqs. (71) and (72) do not contain the Kais constant even though they evaluate type-a integrals. We use such continued fraction expressions in Sect. 5 when we want $\bar{M}(p, q; \ell)$ expressed as an explicit analytic function of ℓ. Other studies of the correlation cusp problem emphasize asymptotic expansions rather than continued fraction expansions. Using Maple it is rather easy to convert almost any formula in this paper into an asymptotic expansion: (1) Wherever an $\bar{M}(p, q; \ell)$ appears in a given expression replace it by a truncated continued fraction with suitably large value of $k_{\max}$. (2) Make the substitution $\ell = 1/y$, or alternatively $\ell = (2 - y)/(2y)$. (3) Expand the resulting expression as a Taylor series in the variable y. The Taylor series coefficients are the desired coefficients in the asymptotic expansion in inverse powers of ℓ, or alternatively, in inverse powers of

$(\ell + 1/2)$. For example, the continued fraction formulas (71) and (72) generate the following asymptotic formula:

$$\bar{M}(2n, -1; \ell) = \Gamma(n + \tfrac{1}{2})\left[\frac{1}{4\ell} - \frac{2n+1}{16\ell^2} + \frac{(2n+1)(2n-1)}{64\ell^3} + O(\ell^{-4})\right]. \quad (73)$$

4.2 Integrals of triple products of Legendre polynomials

We introduce the following three-index notation to denote the integral over a product of three Legendre polynomials [11, 51–53]:

$$[\ell_1, \ell_2, \ell_3] \equiv \int_{-1}^{1} P_{\ell_1}(x) P_{\ell_3}(x) P_{\ell_3}(x)\, dx \quad (74)$$

$$= 2\begin{pmatrix} \ell_1 & \ell_2 & \ell_3 \\ 0 & 0 & 0 \end{pmatrix}^2 \quad (75)$$

$$= 0 \quad \text{when } \ell_1 + \ell_2 + \ell_3 \quad \text{is odd.} \quad (76)$$

Equation (75) shows the relationship to a Wigner 3-j symbol. If the sum of indices is an even integer then $[\ell_1, \ell_2, \ell_3]$ can be evaluated using a formula due to Racah [51]:

$$[\ell_1, \ell_2, \ell_3] = \frac{2(L!)^2 (2L - 2\ell_1)!\,(2L - 2\ell_2)!\,(2L - 2\ell_3)!}{[(L - \ell_1)!\,(L - \ell_2)!\,(L - \ell_3)!]^2\,(2L + 1)!}, \quad (77)$$

$$L \equiv \frac{(\ell_1 + \ell_2 + \ell_3)}{2} = \text{integer}, \quad (78)$$

$$L \geqslant \max(\ell_1, \ell_2, \ell_3). \quad (79)$$

When computing with large angular momentum quantum numbers it is best to recast this in terms of $h(n)$ to avoid integer overflow problems:

$$[\ell_1, \ell_2, \ell_3] = \frac{2\,h(L - \ell_1)\,h(L - \ell_2)\,h(L - \ell_3)}{(2L + 1)\,h(L)}, \quad (80)$$

$$h(n) = [(2n - 1)/(2n)]\,h(n - 1), \quad (81)$$

$$h(0) = 1. \quad (82)$$

As n increases, $h(n)$ decreases approximately as $1/\sqrt{n\pi}$. More precisely, it is given by a terminated continued fraction formula [54]:

$$h(n) \cong \sqrt{\frac{4}{\pi(4n + 1 + 1/(2b_2))}}, \quad (83)$$

$$b_k = \begin{cases} 4n + 1 + (2k - 1)^2/(4b_{k+1}), & k < k_{\max}, \quad (84) \\ 4n + 1, & k = k_{\max}, \quad (85) \end{cases}$$

Equations (83)–(85) are numerically stable, provide an upper or lower bound on the true value of $h(n)$ when $k_{\max}$ is odd or even, respectively, and become exact in the $k_{\max} \to \infty$ limit. True values $h(2) = 3/8$ and $h(10) = 46\,189/262\,144$ are recovered to 10 and 23 significant figures, respectively, when $k_{\max} = 10$, and to 28 and

100 significant figures, respectively, when $k_{\max} = 1000$. We use Eq. (81) for numerical computation and Eq. (83) to generate large-n asymptotic expansions.

5 Partial wave analysis

A two-electron ^1S function can be expressed as follows using coordinates r_1, r_2 and θ_{12}:

$$\Psi(1,2) = \sum_{\ell=0}^{\infty} \Psi^{(\ell)}(r_1, r_2), \tag{86}$$

$$\Psi^{(\ell)}(r_1, r_2) = f_\ell(r_1, r_2) P_\ell(\cos\theta_{12}), \tag{87}$$

$$f_\ell(r_1, r_2) = f_\ell(r_2, r_1), \tag{88}$$

$$f_\ell(r_1, r_2) = \sum_{\nu=1}^{\infty} c_{\nu,\ell} R_{\nu,\ell}(r_1) R_{\nu,\ell}(r_2), \tag{89}$$

$$\delta_{\nu\mu} = \int_0^\infty R_{\nu,\ell}(r) R_{\mu,\ell}(r) r^2 \, dr. \tag{90}$$

We refer to $\Psi^{(\ell)}$ as the ℓth partial wave, and to $f_\ell(r_1, r_2)$ as its amplitude. The natural orbital expansion of the ℓth partial wave amplitude is shown in Eq. (89) where $R_{\nu,\ell}$ is the radial factor of a normalized natural orbital, $R_{\nu,\ell} Y_{\ell m}$. For the Kais function, the f_ℓ are given by simple, closed-form formulas, and the $c_{\nu,\ell}$ and $R_{\nu,\ell}$ can be computed numerically with virtually unlimited precision. In this section we investigate a number of properties of the Kais function which can be expressed as integrals over partial wave amplitudes. The natural orbital expansion and related properties will be treated in the second paper in this series. We compare results for the model system with those reported for the helium atom. The hydride ion would have been a better real system for comparison but for the fact that far more extensive results are available in the literature for helium. In particular, in 1979 Carroll et al. [34] reported extensive configuration interaction calculations for the helium atom ground state. Using piecewise-polynomial radial functions to overcome numerical problems due to near redundancy of traditional orbital basis functions, they were able to nearly saturate the orbital subspaces with angular momentum as high as $L = 11$. The resulting variational energy was only 23 μH above the limit. Decleva et al. [36] recently introduced a number of improvements and further reduced the variational energy error to 78 nano-Hartrees using orbitals with angular momenta as high as $L = 80$.

5.1 Partial waves of the Kais function

Let r_{12} be expanded in Legendre polynomials [53, 55]:

$$r_{12} = \sum_{\ell=0}^{\infty} B_\ell(r_1, r_2) P_\ell(\cos\theta_{12}), \tag{91}$$

$$B_\ell(r_1, r_2) = \frac{r_>^{\ell+2}}{(2\ell+3) r_>^{\ell+1}} - \frac{r_>^{\ell}}{(2\ell-1) r_>^{\ell-1}}, \tag{92}$$

$$r_> = \max(r_1, r_2), \qquad r_< = \min(r_1, r_2). \tag{93}$$

Substitution of Eq. (91) into Eq. (24) yields the partial wave amplitudes for the Kais function:

$$f_\ell(r_1, r_2) = (N/2)[2\delta_{\ell 0} + B_\ell(r_1, r_2)] \exp(-(r_1^2 + r_2^2)/4). \tag{94}$$

Inspection of ((66)) reveals that the following inequalities apply for all finite r_1 and r_2:

$$f_0(r_1, r_2) > 0, \tag{95}$$

$$f_\ell(r_1, r_2) \leqslant 0 \quad \text{when } \ell > 0. \tag{96}$$

As shown in Figs. 4 and 5, $-f_\ell(r_1, r_2)$ has a sharp ridge extending along the diagonal, $r_1 = r_2$, and this ridge becomes increasingly sharp as ℓ increases. All amplitudes with $\ell > 0$ have their maximum absolute values at the same point, namely, when $r_1 = r_2 = 1$ Bohr, and their values at this point decrease with increasing ℓ as ℓ^{-2}. Viewed along this ridge, all amplitudes with $\ell > 0$ have precisely the same functional dependence on r_1:

$$f_0(r_1, r_1) = N(1 + 2r_1/3)\exp(-r_1^2/2), \tag{97}$$

$$f_\ell(r_1, r_1) = \frac{-2Nr_1 \exp(-r_1^2/2)}{(2\ell + 3)(2\ell - 1)} \quad \text{when } \ell > 0. \tag{98}$$

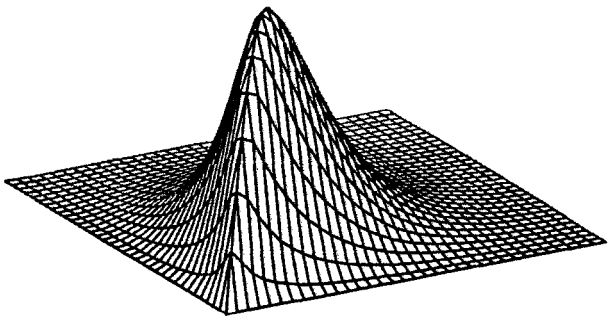

Fig. 4. Negative partial wave amplitude, $-f_2(r_1, r_2)$, for the Kais function. The maximum absolute value occurs at $r_1 = r_2 = 1$ Bohr

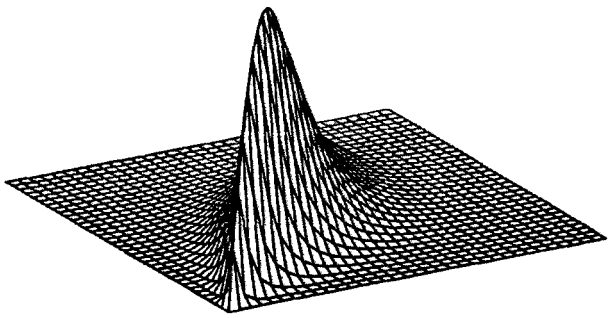

Fig. 5. Negative partial wave amplitude, $-f_5(r_1, r_2)$, viewed from the same perspective as the $\ell = 2$ function shown in Fig. 4. Both functions peak at the same point, but the $\ell = 5$ function exhibits a sharper ridge

These amplitudes bear a remarkable resemblance to those computed for the helium atom. The three-dimensional plots of partial wave amplitudes for the model, shown in Figs. 4 and 5, can hardly be distinguished by the human eye from those for the helium atom, shown in Figs. 6 and 7 in the 1995 paper of Decleva et al. [36]. Readers of that paper should note that the function plotted there is $r_1 r_2 f_\ell(r_1, r_2)$ not $f_\ell(r_1, r_2)$ as indicated in the figure captions [56]. Figures 8 and 9 in that paper show plots of $r^2 f_\ell(r, r)$ for various ℓ rescaled so that each plot has unit maximum amplitude. In agreement with (98), these various functions of r are nearly identical for all $\ell > 0$ showing small departures from one another mainly in the diffuse tail regions. The $\ell = 0$ function exhibits a maximum at $r \approx 0.6$. All higher angular momentum functions have their maxima at $r \approx 0.8$. The corresponding values for the model, implied by (97, 98), are $r = 1.586$ for $\ell = 0$ and $r = 1.732$ for all higher ℓ. Numerical values of these distances for the model are about twice the corresponding helium atom values as one would expect for the more diffuse charge distribution. Otherwise, partial wave expansions for the two systems exhibit the same qualitative features.

Earlier analyses by Hill [11] and others [32, 33] show that the squared norm of a helium atom partial wave, $\langle \Psi^{(\ell)} | \Psi^{(\ell)} \rangle$, decreases with increasing ℓ as the inverse sixth power of ℓ. The same is true of partial waves of the Kais function. Four powers of ℓ come from the denominator in (98), an additional power of ℓ comes from angular averaging, and one more power of ℓ comes from decreasing thickness, i.e. from the fact that the high angular momentum f_ℓ functions peak more sharply about the ridge line. The r_1^2 operator is an example of an operator that is not particularly sensitive to the correlation cusp region. It comes as no surprise that matrix elements $\langle \Psi^{(\ell)} | r_1^2 | \Psi^{(\ell)} \rangle$ also exhibit inverse-sixth-power dependence on ℓ. If, however, an operator is particularly sensitive to the partial wave amplitude in the immediate vicinity of the ridge line then one might expect its matrix elements to be of order $O(\ell^{-n})$ where $n < 6$. Earlier studies show that $n = 4$ for the kinetic energy and r_{12}^{-1} operators. Such integrals over Kais partial waves are discussed in detail below.

5.2 Partial wave norm

The norm and similar integral properties of the partial waves can be calculated using methods discussed in Sect. 4. Consider the integral over six-dimensional space of a symmetric function $F(r_1, r_2, \theta_{12}) = F(r_2, r_1, \theta_{12})$:

$$\int \cdots \int F(r_1, r_2, \theta_{12}) \mathrm{d}^3 \boldsymbol{r}_1 \, \mathrm{d}^3 \boldsymbol{r}_2 = 16\pi^2 \int_0^\infty \mathrm{d}r_1 \int_{r_2 = r_1}^\infty \mathrm{d}r_2 \int_0^\pi \mathrm{d}\theta_{12} \, r_1^2 r_2^2 \sin\theta_{12} \, F(r_1, r_2, \theta_{12}). \tag{99}$$

The factor of $16\pi^2$ consists of a factor of $8\pi^2$ coming from integration over the three complementary angular coordinates and an additional factor of 2 that compensates for the fact that we integrate only over the half-space $r_1 \leqslant r_2$. The squared norm is an example of (99) with integrand $F = [\Psi^{(\ell)}]^2$. As stated above, the angular integration in (99) contributes one factor of $(\ell + \frac{1}{2})^{-1}$:

$$\int_0^\pi P_\ell(\cos\theta) \, P_{\ell'}(\cos\theta) \sin\theta \, \mathrm{d}\theta = 2\delta_{\ell\ell'}/(2\ell + 1). \tag{100}$$

Note that partial waves are orthogonal by virtue of their angular factors. The squared norm reduces to a two-dimensional integral:

$$\langle \Psi^{(\ell)} | \Psi^{(\ell)} \rangle = \frac{8\pi^2 N^2}{(2\ell+1)} \int_0^\infty dx \int_{y=x}^\infty dy \exp(-(x^2+y^2)/2)\, x^2 y^2 [2\delta_{\ell 0} + B_\ell(x,y)]^2, \tag{101}$$

$$B_\ell(x,y) = (2\ell+3)^{-1} x^{\ell+2} y^{-1-\ell} - (2\ell-1)^{-1} x^\ell y^{1-\ell}. \tag{102}$$

The significance of the squared norm of the ℓth partial wave is that it equals half the sum of all ℓ-type natural orbital occupation numbers. The integral in (101) is in standard form, and so can be expressed as a linear combination of $M(p, q)$ integrals. Although the $\ell = 0$ case is in standard form, it requires special attention because of the Kronecker delta term. Normalization of Ψ implies the following:

$$\langle \Psi | \Psi \rangle = \sum_{\ell=0}^{\infty} \langle \Psi^{(\ell)} | \Psi^{(\ell)} \rangle = 1. \tag{103}$$

The sum is dominated by the contribution of the $\ell = 0$ wave:

$$\langle \Psi^{(0)} | \Psi^{(0)} \rangle = \frac{8(6\pi + 9\sqrt{\pi} - 2)}{9(5\pi + 8\sqrt{\pi})} \tag{104}$$

$$= 0.9755557364. \tag{105}$$

The B_ℓ^2 factor in (101) generates a linear combination of three b-type $M(p, q)$ integrals when $\ell > 0$. Using the recurrence formula (65) these reduce to a single $\bar{M}(6, 0; \ell)$ integral:

$$\langle \Psi^{(\ell)} | \Psi^{(\ell)} \rangle = c_\ell \left[\frac{-24(2\ell-5)}{(2\ell-1)} + \frac{8(4\ell^2+4\ell-5)\bar{M}(6,0,\ell)}{(2\ell+3)} \right], \tag{106}$$

$$c_\ell = [(2\ell+5)(2\ell+3)(2\ell+1)(2\ell-1)(5\pi + 8\sqrt{\pi})]^{-1}. \tag{107}$$

Substituting computer-generated formulas [31, 57] for b-type $\bar{M}$ integrals yields the following exact formula:

$$\langle \Psi^{(\ell)} | \Psi^{(\ell)} \rangle = \frac{2|\alpha_\ell - \beta_\ell \pi|}{(5\pi + 8\sqrt{\pi})} \quad \text{when } \ell > 0. \tag{108}$$

Here α_ℓ and β_ℓ are positive rational numbers that increase monotonically with increasing ℓ to π and 1, respectively. Only β_ℓ has a simple closed-form formula:

$$\beta_\ell = 1 - \frac{2}{(2\ell-1)(2\ell+3)}. \tag{109}$$

The first α_ℓ value is $\alpha_1 = 56/25$. Higher values can be computed using the following recurrence relation derived from (65):

$$\alpha_\ell = \frac{(2\ell+3)(2\ell+1)(2\ell-3)^2(4\ell^2+4\ell-5)\alpha_{\ell-1} + (-1)^{\ell-1}240}{(2\ell+3)^2(2\ell-1)(2\ell-3)(4\ell^2-4\ell-5)}. \tag{110}$$

Table 2. Rational numbers that appear in the exact formula (108) for the square of the norm of the partial waves of the Kais function

ℓ	α_ℓ		β_ℓ
	Exact	Numerical	
1	56/25	2.2400000	3/5
2	6248/2205	2.8335601	19/21
3	42568/14175	3.0030335	43/45
4	54424/17787	3.0597627	75/77
5	3254872/1054053	3.0879586	115/117
6	4613288/1486485	3.1034878	163/165
7	35123656/11282271	3.1131725	245/247

The first seven α_ℓ and β_ℓ values are reported in Table 2. The asymptotic expansion is obtained [50] by the method described at the end of Sect. 4:

$$\langle \Psi^{(\ell)} | \Psi^{(\ell)} \rangle = (15/4) C_1 [2(\ell + \tfrac{1}{2})^{-6} + 21(\ell + \tfrac{1}{2})^{-10} - 187(\ell + \tfrac{1}{2})^{-12} + O(\ell^{-14})]. \tag{111}$$

The first term in (111) provides a lower bound and the sum of the first two terms provides an upper bound on the true value for all $\ell > 0$. The $\ell = 0$ case is entirely anomalous in this respect. As found in earlier studies [11, 32, 33], odd-power terms are eliminated by expanding in inverse powers of $(\ell + 1/2)$ rather than ℓ itself. The c_ℓ factor of order $O(\ell^{-4})$ is multiplied in (106) by the sum of two terms whose large-ℓ limiting values are -24 and 24, respectively. Near cancellation of these two terms yields the leading inverse-sixth-power term in (111). Absence of an inverse-eighth-power term appears to be a special result for the Hooke's law model.

5.3 Mean-squared-radius

Consider the squared radius, r_1^2, averaged over a partial wave:

$$\langle \Psi^{(\ell)} | r_1^2 | \Psi^{(\ell)} \rangle = \langle \Psi^{(\ell)} | \tfrac{1}{2}(r_1^2 + r_2^2) | \Psi^{(\ell)} \rangle \tag{112}$$

$$= \frac{4\pi^2 N^2}{(2\ell + 1)} \int_0^\infty dx \int_{y=x}^\infty dy (x^2 + y^2) \exp(-\tfrac{1}{2}(x^2 + y^2)) x^2 y^2 \times [2\delta_{\ell 0} + B_\ell(x, y)]^2. \tag{113}$$

The integrand is symmetrized in (112) to bring (113) into standard form. The $\ell = 0$ case reduces to

$$\langle \Psi^{(0)} | r_1^2 | \Psi^{(0)} \rangle = \frac{174\pi + 252\sqrt{\pi} - 64}{45\pi + 72\sqrt{\pi}} \tag{114}$$

$$= 3.454779747 \tag{115}$$

$$= 3.541345325 \langle \Psi^{(0)} | \Psi^{(0)} \rangle. \tag{116}$$

If $\ell > 0$ then Eq. (113) reduces to a linear combination of six type-b $M(p, q)$ integrals. When Maple was instructed to simplify this rather complicated expression it produced the following remarkably simple result:

$$\langle \Psi^{(\ell)} | r_1^2 | \Psi^{(\ell)} \rangle = 4 \; < \Psi^{(\ell)} \; | \Psi^{(\ell)} \; > \quad \text{when } \ell > 0. \tag{117}$$

The following infinite series can be summed exactly making use of (117) and (103):

$$\sum_{\ell=0}^{\infty} \langle \Psi^{(\ell)} | r_1^2 | \Psi^{(\ell)} \rangle = \langle \Psi^{(0)} | r_1^2 | \Psi^{(0)} \rangle + 4 \sum_{\ell=1}^{\infty} \langle \Psi^{(\ell)} | \Psi^{(\ell)} \rangle, \tag{118}$$

$$\langle \Psi | r_1^2 | \Psi \rangle = \langle \Psi^{(0)} | r_1^2 | \Psi^{(0)} \rangle + 4(1 - \langle \Psi^{(0)} | \Psi^{(0)} \rangle). \tag{119}$$

The known result (39) is recovered when (104) and (114) are substituted into (119).

5.4 Kinetic energy

Let T_ℓ be the matrix element of the kinetic energy operator:

$$T_\ell \equiv \langle \Psi^{(\ell)} | -\tfrac{1}{2}(\nabla_1^2 + \nabla_2^2) | \Psi^{(\ell)} \rangle. \tag{120}$$

The Legendre polynomial factor $P_\ell(\cos\theta_{12})$ is an eigenfunction of the Laplacian operator:

$$\nabla_1^2 P_\ell(\cos\theta_{12}) = \frac{-\ell(\ell+1)}{r_1^2} P_\ell(\cos\theta_{12}). \tag{121}$$

So T_ℓ can be partitioned into its radial and angular components:

$$T_\ell = Tr_\ell + Ta_\ell, \tag{122}$$

$$Ta_\ell = \frac{\ell(\ell+1)}{2} \left\langle \Psi^{(\ell)} \middle| \left(\frac{1}{r_1^2} + \frac{1}{r_2^2} \right) \middle| \Psi^{(\ell)} \right\rangle, \tag{123}$$

$$Tr_\ell = \frac{-4\pi^2 N^2}{(2\ell+1)} \int_0^\infty \int_0^\infty dx\, dy\, xy f_\ell(x, y) \frac{\partial^2 xy f_\ell(x, y)}{\partial x^2}, \tag{124}$$

$$= \frac{4\pi^2 N^2}{(2\ell+1)} \int_0^\infty \int_0^\infty dx\, dy \left[\frac{\partial xy f_\ell(x, y)}{\partial x} \right]^2 \tag{125}$$

$$= \frac{4\pi^2 N^2}{(2\ell+1)} \int_0^\infty dx \int_{y=x}^\infty dy \left\{ \left[\frac{\partial xy f_\ell(x, y)}{\partial x} \right]^2 + \left[\frac{\partial xy f_\ell(x, y)}{\partial y} \right]^2 \right\}. \tag{126}$$

The integrand in (124) contains the radial component of a one-particle Laplacian operator expressed in polar coordinates. Recall that $B_\ell(x, y)$ has a discontinuous first derivative at $x = y$. To avoid taking the second derivative, we use the Hermitian property in (125) to convert to a product of first derivatives. In (126) we restore the symmetry of the integrand. Now Eqs. (123) and (126) are both in standard form and so reduce to the usual linear combination of $M(p, q)$ integrals. Again we relegate all manipulations to Maple, namely, perform the differentiations in (126), generate the list of $M(p, q)$ factors, reduce the number of terms using

recurrence relations, and simplify the resulting algebraic expression. The result in the special case $\ell = 0$ is,

$$T_0 = \frac{51\pi + 90\sqrt{\pi} + 16}{18(5\pi + 8\sqrt{\pi})} \tag{127}$$

$$= 0.6240829316. \tag{128}$$

The following formulas are exact for all $\ell > 0$:

$$T_\ell = \frac{4\,|\alpha_\ell' - \pi|}{(2\ell - 1)(2\ell + 3)(5\pi + 8\sqrt{\pi})}, \tag{129}$$

$$\alpha_\ell' = \frac{-2}{3} + 12 \sum_{k=1}^{k=\ell} \frac{(-1)^k}{4k^2 - 9}, \tag{130}$$

$$\alpha_\infty' = \pi. \tag{131}$$

Here α_ℓ' is a positive rational number expressed as a finite series which can be summed explicitly. For very large ℓ the series can be evaluated in terms of a polygamma function [58]. As shown in Table 3, α_ℓ' oscillates about π and converges to π in the $\ell \to \infty$ limit. To check the lengthy manipulations carried out by Maple, T_ℓ was evaluated by Eqs. (127)–(130), summed numerically, and compared with (43). Agreement is observed to 4, 7 and 10 significant figures when the sum is carried out to 10, 100 and 1000 terms, respectively. The following asymptotic expansion is obtained using methods described in Sect. 4:

$$T_\ell = \tfrac{3}{2} C_1 [2(\ell + \tfrac{1}{2})^{-4} + 5(\ell + \tfrac{1}{2})^{-6} + 7(\ell + \tfrac{1}{2})^{-8} + \tfrac{25}{2}(\ell + \tfrac{1}{2})^{-10} + \cdots]. \tag{132}$$

As in earlier studies [11, 33, 32] we obtain an expansion in inverse even powers of $(\ell + \frac{1}{2})$ with the leading term being inverse-fourth-power. The presence of an inverse-fourth-power term and absence of an inverse-fifth-power term is significant for the discussion in Sect. 5.7 of an approximate virial relation.

Table 3. The rational number that appears in the exact formula (129) for the kinetic energy of a partial wave of the Kais function

ℓ	α_ℓ'	
	Exact	Numerical
1	26/15	1.7333333
2	362/105	3.4476190
3	946/315	3.0031746
4	11162/3465	3.2213564
5	139166/45045	3.0894883
6	28634/9009	3.1783772
7	476950/153153	3.1142061

5.5 *Potential energy*

Here we compute the matrices of potential energy operators in a basis of partial waves. In effect, the diagonal matrix of one-particle operators was computed in Sect. 5.3.

$$V^{(1)}_{\ell,\ell'} = \delta_{\ell',\ell} \langle \Psi^{(\ell)} | \tfrac{1}{2} k (r_1^2 + r_2^2) | \Psi^{(\ell)} \rangle \tag{133}$$

$$= \delta_{\ell',\ell} < \Psi^{(\ell)} | \Psi^{(\ell)} > \quad \text{when } \ell > 0. \tag{134}$$

The analogous two-particle matrix, $V^{(2)}$, consists of electron-repulsion integrals:

$$V^{(2)}_{\ell,\ell'} \equiv \langle \Psi^{(\ell)} | r_{12}^{-1} | \Psi^{(\ell')} \rangle. \tag{135}$$

Substituting the Legendre expansion [55] of r_{12}^{-1} into (135) and performing the angular integration in (99) using (74) yields a finite sum of two-dimensional radial integrals:

$$V^{(2)}_{\ell,\ell'} = 16\pi^2 \sum_{\ell''}{}' [\ell, \ell', \ell''] \int_0^\infty dr_1 \int_{r_2=r_1}^\infty dr_2 r_1^{2+\ell''} r_2^{1-\ell''} f_\ell(r_1, r_2) f_{\ell'}(r_1, r_2). \tag{136}$$

The prime on the summation symbol indicates that the summation index is incremented in steps of two over the following limits:

$$\ell'' = |\ell - \ell'|, |\ell - \ell'| + 2, \ldots, \ell + \ell'. \tag{137}$$

Each integrand in (136) is everywhere non-negative except when one and only one of the indices ℓ and ℓ' is zero, and then the integrand is everywhere non-positive. Thus the Hamiltonian matrix has the block structure shown in Fig. 6. When either or both indices of $V^{(2)}_{\ell,\ell'}$ are zero, the summation in (136) consists of a single term. In the special case $\ell = \ell' = 0$ the result is

$$V^{(2)}_{0,0} = \frac{-48 + 20\sqrt{\pi} + 30\chi + 36\pi}{45\pi + 72\sqrt{\pi}} \tag{138}$$

$$= 0.4969938419. \tag{139}$$

The exact formula for $\ell > 0$, $\ell' = 0$ is

$$V^{(2)}_{\ell,0} = 8\pi^2 N^2 [A(\ell) + B(\ell)\sqrt{\pi} + C(\ell)\chi + (-1)^\ell \pi], \tag{140}$$

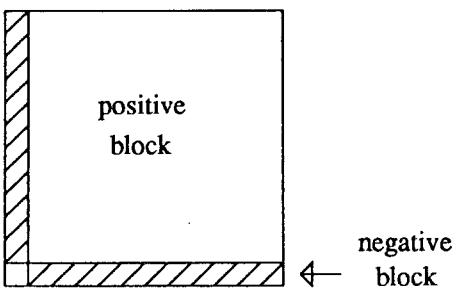

Fig. 6. Block structure of the Hamiltonian matrix in the partial wave basis. The small diagonal block consists of a single matrix element. Elements in diagonal blocks are all positive. Those in off-diagonal blocks are all negative

Table 4. Rational numbers that appear in the exact formula (140) for the $V^{(2)}_{\ell,0}$ electron repulsion integral

ℓ	$A(\ell)$	$B(\ell)$	$C(\ell)$
1	44/15	91/90	−11/6
2	−332/105	59/504	−5/24
3	988/315	−10453/15120	53/48
4	−1556/495	286903/266112	−665/384
5	141476/45045	−1376095/988416	1715/768

where $A(\ell)$, $B(\ell)$ and $C(\ell)$ are rational numbers given by Eqs. (141)–(149) and listed in Table 4.

$$A(\ell) = \frac{-24}{a1(\ell)(2\ell-3)} - A(\ell-1), \tag{141}$$

$$a1(\ell) = (2\ell+3)(2\ell+1)(2\ell-1), \tag{142}$$

$$A(1) = 44/15, \tag{143}$$

$$B(\ell) = -\frac{b1(\ell) + b2(\ell)\,B(\ell-1)}{b3(\ell)}, \tag{144}$$

$$b1(\ell) = 240\ell^2 - 540\ell + 130, \tag{145}$$

$$b2(\ell) = a1(\ell)(2\ell-3)(16\ell^2 - 32\ell + 5), \tag{146}$$

$$b3(\ell) = a1(\ell)(32\ell^3 - 128\ell^2 + 106\ell), \tag{147}$$

$$B(\ell) = 91/90, \tag{148}$$

$$C(\ell) = \frac{(-1)^{\ell+1}(16\ell^2 - 32\ell + 5)(2\ell)!}{3(2\ell-1)(\ell!)^2\,4^\ell}. \tag{149}$$

The absolute value of this matrix element falls off as the inverse fourth power of ℓ:

$$V^{(2)}_{\ell,0} = \frac{-3}{16\sqrt{\pi}(\ell+1/2)^4} + \frac{-25}{256(5\sqrt{\pi}+8)(\ell+1/2)^6} + O(\ell^{-7}). \tag{150}$$

Numerical results obtained with the above asymptotic expansion are compared with exact values in Table 5.

Now consider matrix elements of Eq. (136) with $\ell > 0$ and $\ell' > 0$. Substitute Eqs. (87) and (94), drop the Kronecker delta term, perform the angular integration using Eq. (74) and the radial integrations using Eqs. (51), (63) and (64) to get

$$V^{(2)}_{\ell,\ell'} = 4\pi^2 N^2 \sum_{\ell''}{}' [\ell, \ell', \ell''](\tau(6, -1)\,\bar{M}(6, -1; L) + \tau(4, 1)\,\bar{M}(6, -1; L-1) + \tau(2, 3)\,\bar{M}(6, -1; L-2)), \tag{151}$$

$$L = (\ell + \ell' + \ell'')/2, \tag{152}$$

$$\tau(6, -1) = (2\ell+3)^{-1}(2\ell'+3)^{-1}, \tag{153}$$

$$\tau(4, 1) = -(2\ell+3)^{-1}(2\ell'-1)^{-1} - (2\ell-1)^{-1}(2\ell'+3)^{-1}, \tag{154}$$

$$\tau(2, 3) = (2\ell-1)^{-1}(2\ell'-1)^{-1}. \tag{155}$$

Table 5. Asymptotic approximations (150) and exact value (140) of the electron repulsion integral $V^{(2)}_{\ell,0}$. Values are reported in atomic units in floating point notation with power of ten in parentheses

ℓ	One term	Two terms	Exact
1	−0.2089591050 (−1)	−0.2140434671 (−1)	−0.2952938673 (−1)
2	−0.2708110001 (−2)	−0.2731831601 (−2)	−0.2874462410 (−2)
3	−0.7049432531 (−3)	−0.7080937260 (−3)	−0.7187866792 (−3)
4	−0.2579742037 (−3)	−0.2586716471 (−3)	−0.2601782535 (−3)
5	−0.1156047231 (−3)	−0.1158139453 (−3)	−0.1161221038 (−3)
10	−0.8703003124 (−5)	−0.8707324761(−5)	−0.8708908890 (−5)
20	−0.5989780277 (−6)	−0.5990560576 (−6)	−0.5990604900 (−6)
30	−0.1222438385 (−6)	−0.1222510327 (−6)	−0.1222510797 (−6)
40	−0.3931934213 (−7)	−0.3932065449 (−7)	−0.3932064499 (−7)
50	−0.1626525301 (−7)	−0.1626560218 (−7)	−0.1626559809 (−7)
100	−0.1036960202 (−8)	−0.1036965823 (−8)	−0.1036965756 (−8)
200	−0.6545891883 (−10)	−0.6545900798 (−10)	−0.6545900731 (−10)
300	−0.1297323934 (−10)	−0.1297324721 (−10)	−0.1297324716 (−10)
400	−0.4111651092 (−11)	−0.4111652495 (−11)	−0.4111652490 (−11)
500	−0.1685815368 (−11)	−0.1685815736 (−11)	−0.1685815735 (−11)

The τ coefficients are products of the denominators in Eq. (102). Again the sum of three a-type $\bar{M}$ integrals can be combined using Eq. (65) leading, eventually, to the following asymptotic expansion valid for $0 < \ell' \leqq \ell$. The finite sum over ℓ'' in Eq. (151) has been performed exactly in obtaining the coefficients in the following expression:

$$V^{(2)}_{\ell,\ell'} = \frac{15C_1}{8(2\ell'+3)\,(2\ell'-1)}\left[\frac{3}{(\ell+\frac{1}{2})^4} + \frac{10(\ell')^2+10\ell'+5}{16(\ell+1/2)^6} + O(\ell^{-7})\right]. \quad (156)$$

Note that these matrix elements are all positive and are of order $O(\ell^{-4}(\ell')^{-2})$ for large values of its indices.

5.6 *Energy convergence rate*

Let $\bar{\Psi}_L$ be the truncated, partial wave expansion of the Kais function and Ψ_L the corresponding, renormalized, approximate wave function. Let $\bar{E}_L$ and E_L be the corresponding energy integrals:

$$\bar{\Psi}_L \equiv \sum_{\ell=0}^{L} \Psi^{(\ell)}(\boldsymbol{r}_1, \boldsymbol{r}_2), \qquad \Psi_L = N_L \bar{\Psi}_L, \quad (157)$$

$$\bar{E}_L = \langle \bar{\Psi}_L | \mathscr{H} | \bar{\Psi}_L \rangle, \qquad E_L = N_L^2 \bar{E}_L. \quad (158)$$

In the infinite L limit $\bar{\Psi}_L$ and Ψ_L both converges to the true ground state wave function, $\Psi_\infty = \Psi(1,2)$, as do $\bar{E}_L$ and E_L to the ground state energy, $E_\infty = 2$ H. Here we investigate the rate of convergence as measured by the energy error ΔE_L:

$$\Delta E_L = E_L - E_\infty. \quad (159)$$

This provides a reliable indication of the rate of convergence of a full-CI calculation using an orbital basis that is complete in ℓ-type subspaces with $\ell \leqslant L$ but totally lacking higher angular momentum orbitals. The FCI convergence rate is a bit faster because the ℓth partial wave of the FCI wave function, $\Psi_L^{(\ell)}(\mathrm{FCI})$, relaxes to compensate, as best it can, for the absence of waves with $\ell > L$. It is thoroughly documented in the helium atom calculations of Carroll et al. [34] that this relaxation effect is remarkably small, and confined almost entirely to the last wave, $\Psi_L^{(L)}(\mathrm{FCI})$:

$$\Psi_L^{(\ell)}(\mathrm{FCI}) \approx \Psi^{(\ell)} \quad \text{when } \ell < L. \tag{160}$$

In fact, the insensitivity of $\Psi_L^{(\ell)}(\mathrm{FCI})$ to the value of L underlies the efficiency of iterative numerical methods devised by Decleva, Lisini and Venuti to diagonalize the large CI matrices in their helium atom CI calculations [36]. The partial wave truncation error for the Kais function, defined in Eq. (159), converges from above to that of the full-CI calculation as L increases (see discussion below), so one expects Eq. (160) to become an equality in the large-L limit. We now present results of a limited variational calculation that suggest that Eq. (160) is a good approximation for the Kais function even for very small L. The chosen variational basis is not very flexible, but it does contain the exact wave function in the infinite basis limit, so it establishes a lower bound (not the more interesting upper bound) on the the magnitude of the relaxation effect. This variational function, denoted Ψ_L (Ritz), treats the renormalized partial waves as variational basis functions whose coefficients are determined by energy minimization rather than by overlap with the true wave function:

$$\Psi_L(\mathrm{Ritz}) = \sum_{\ell=0}^{L} c'_{L,\ell}\, \Psi^{(\ell)}(\boldsymbol{r}_1, \boldsymbol{r}_2). \tag{161}$$

Matrix elements of the Hamiltonian in the partial wave basis are computed numerically using exact formulas given above:

$$H_{\ell',\ell} = \delta_{\ell',\ell}(T_\ell + V^{(1)}_{\ell,\ell}) + V^{(2)}_{\ell',\ell}. \tag{162}$$

For example,

$$H_{0,0} = \frac{105\pi + 128\sqrt{\pi} - 56 + 30\chi}{45\pi + 72\sqrt{\pi}} \tag{163}$$

$$= 1.9847717102. \tag{164}$$

The truncated partial wave energy, E_L, is computed as a sum of Hamiltonian matrix elements:

$$\sigma_\ell \equiv \sum_{\ell'=0}^{\ell} (2 - \delta_{\ell,\ell'}) H_{\ell',\ell}, \tag{165}$$

$$E_L = N_L^2 \sum_{\ell=0}^{\ell=L} \sigma_\ell. \tag{166}$$

The significance of σ_ℓ is that it is the ℓth energy increment to the energy $\bar{E}_L$ computed with the nonormalized wave function $\bar{\Psi}_L$. The renormalization correction is negligible for all but the smallest L values, see discussion below, so σ_ℓ measures the energy contribution from ℓ-type orbitals. The energy, $E_L(Ritz)$, is the lowest eigenvalue of the symmetric matrix, $\bar{H}$, with renormalized elements:

$$\bar{H}_{\ell',\ell} = H_{\ell',\ell}\langle\Psi^{(\ell')}|\Psi^{(\ell')}\rangle\langle\Psi^{(\ell)}|\Psi^{(\ell)}\rangle)^{-1/2}. \tag{167}$$

This matrix has the block structure shown in Fig. 6. Table 6 reports numerical values of relevant matrix elements. Sums of elements with $\ell \leqslant 15$ are compared with limiting values obtained from Eqs. (103), (43), (27) and (28). Note that σ_ℓ is negative for all $\ell > 1$, due to the dominant contribution of the $\ell' = 0$ term in Eq. (165), and is approximately equal to $-T_\ell$ for large ℓ. Table 7 reports ΔE_L, ΔE_L(Ritz), and the ratio ΔE_L(Ritz)/ΔE_L for $L \leqslant 15$. The largest observed relaxation effect is a 3% reduction when $L = 1$. The effect decreases monotonically with increasing L. For example, relaxation reduces the energy error by only 1% when $L = 3$. The near equality in (160), and all other evidence, supports the claim that the rate of decay of ΔE_L with increasing L is a meaningful measure of convergence rate.

Hill's analysis of variational convergence yields the asymptotic formula (8) for the energy truncation error in the limit of large L where the coefficients C_1 and C_2 are given by appropriate integrals over the exact wave function [59]. Independent formal analysis of the Kais function in Sect. 5.7 below shows that ΔE_L satisfies precisely the same equation. The C_1 and C_2 integrals for the Kais function are evaluated in (47) and (49). It is shown in Table 8 that Hill's one-term and two-term

Table 6. Values of diagonal elements of the overlap and kinetic energy matrices, and partial sums of Hamiltonian matrix elements computed in the partial wave basis using exact formulas. The last two rows report the sum of terms through $\ell = 15$, and the infinite series limit. Values are reported in atomic units in floating point notation with power of ten in parentheses

ℓ	$\langle\Psi^{(\ell)}\|\Psi^{(\ell)}\rangle$	T_ℓ	σ_ℓ	σ_ℓ/T_ℓ
0	0.9755557364 (0)	0.6240829316 (0)	0.1984771710 (1)	3.189
1	0.2375864761 (−1)	0.3769481924 (−1)	0.1655707021 (−1)	0.439
2	0.5910989371 (−3)	0.1950332354 (−2)	−0.7842323726 (−3)	−0.402
3	0.7141399654 (−4)	0.4116700285 (−3)	−0.2930964678 (−3)	−0.712
4	0.1539744756 (−4)	0.1386385382 (−3)	−0.1179661565 (−3)	−0.851
5	0.4574478026 (−5)	0.5960151148 (−4)	−0.5493425468 (−4)	−0.922
6	0.1671904665 (−5)	0.2983666244 (−4)	−0.2867536639 (−4)	−0.961
7	0.7070209394 (−6)	0.1658497617 (−4)	−0.1632591838 (−4)	−0.984
8	0.3332811345 (−6)	0.9953738696 (−5)	−0.9941622497 (−5)	−0.999
9	0.1708877940 (−6)	0.6335161959 (−5)	−0.6385593603 (−5)	−1.008
10	0.9370288599 (−7)	0.4223818977 (−5)	−0.4282634424 (−5)	−1.014
11	0.5427479828 (−7)	0.2924344082 (−5)	−0.2976507902 (−5)	−1.018
12	0.3290465198 (−7)	0.2088891743 (−5)	−0.2131510473 (−5)	−1.020
13	0.2073331730 (−7)	0.1531890497 (−5)	−0.1565683515 (−5)	−1.022
14	0.1350303457 (−7)	0.1148936765 (−5)	−0.1175470468 (−5)	−1.023
15	0.9049537239 (−8)	0.8786089207 (−6)	−0.8994276170 (−6)	−1.024
Sum	0.9999999762	0.6644135003	2.0000041914	
Limit	1.0000000000	0.6644176006	2.0000000000	

Table 7. Energy error due to truncating the partial wave expansion of the Kais function after $\ell = L$. Energy errors are reported for expansion coefficients determined by overlap with the true wave function (column 2), or determined by energy minimization (column 3). Energies are reported in μH units

L	ΔE_L	ΔE_L (Ritz)	Ratio
0	34503.654	34503.654	1.000
1	2701.865	2622.289	0.971
2	733.651	721.799	0.984
3	297.664	294.644	0.990
4	148.898	147.858	0.993
5	84.814	84.381	0.995
6	52.794	52.588	0.996
7	35.054	34.946	0.997
8	24.446	24.385	0.998
9	17.719	17.682	0.998
10	13.249	13.225	0.998
11	10.164	10.148	0.998
12	7.966	7.956	0.999
13	6.359	6.352	0.999
14	5.157	5.151	0.999
15	4.239	4.235	0.999

Table 8. Comparison of five different estimates of ΔE_L. Hill's one-term formula (column 2) provides a lower bound for all L for the Kais function, and Hill's two-term formula (column 4) an upper bound. Results using improved two-parameter formulas are reported in columns 5 and 6. Column 7 reports results using an 8-parameter continued fraction formula. Energies are reported in μH units

L	Hill One-term	Kais ΔE_L	Hill Two-term	Eq. (168)	Eq. (171)	Eq. (172)
0	16729.349	34503.654	∞	34134.334	27347.689	23732.150
1	2091.169	2701.865	12709.509	2924.583	2754.815	2595.409
2	619.606	733.651	1283.252	771.614	750.696	726.530
3	261.396	297.664	392.487	307.682	302.874	296.677
4	133.835	148.898	175.313	152.370	150.824	148.691
5	77.451	84.814	94.440	86.258	85.644	84.757
6	48.774	52.794	56.967	53.478	53.196	52.775
7	32.675	35.054	37.097	35.410	35.267	35.047
8	22.948	24.446	25.541	24.646	24.567	24.442
9	16.729	17.719	18.348	17.838	17.791	17.717
10	12.569	13.249	13.631	13.323	13.294	13.247
11	9.681	10.164	10.407	10.212	10.193	10.162
12	7.615	7.966	8.127	7.999	7.986	7.968
13	6.097	6.359	6.468	6.382	6.373	6.359
14	4.957	5.157	5.233	5.173	5.167	5.157
15	4.084	4.239	4.294	4.251	4.246	4.239

formulas provide lower and upper bounds, respectively, on the value of ΔE_L for all L for the Kais function. (It is not known if this result extends to other systems). Inspection of Table 8 shows, however, that the two-term formula seriously over estimates truncation errors for $L < 6$, which is the range of greatest practical

interest. Column 5 in Table 8 reports an alternative estimate given by the leading term in Eq. (9).

$$\Delta E_L \approx C_1 (L + \bar{C}_2)^{-3}, \tag{168}$$

$$\bar{C}_2 \equiv 1 - C_2/(3C_1) \tag{169}$$

$$= 1 - 3/(8\sqrt{\pi}) \quad \text{for Kais function.} \tag{170}$$

The theoretical justification for (168) is neither greater nor less than that for (8), since they differ only by unspecified terms of order $O(L^{-5})$. It is shown in Table 8 that the simple inverse-third-power formula (168) provides a better estimate of ΔE_L for the Kais function for all L, and significantly better for low L. Column 6 in Table 8 reports yet another modified version of Hill's two-term formula that yields an even lower, thus slightly better, estimate for the Kais function.

$$\Delta E_L \approx C_1 (L + 1)^{-3} + C_2 (L + 1)^{-4}. \tag{171}$$

Either of these these two modifications of Hill's two-term formula is generally preferable to the original from which they were obtained. Both modifications avoid the singularity at $L = 0$ which has has no physical basis.

The first modification, (168), can be thought of as a continued fraction terminated with $\bar{C}_3 = 0$:

$$\Delta E_L = \frac{C_1}{(L + \bar{C}_2 + \bar{C}_3/(L + \bar{C}_4 + \cdots))^3}. \tag{172}$$

All such expansions appear to be well behaved for all nonnegative L. Column 7 in Table 8 reports values of the continued fraction terminated with $\bar{C}_9 = 0$. The parameter values, reported in Table 9, were obtained by a least squares fit (logarithmic) of numerical ΔE_L values. We estimate that the reported values of $\bar{C}_3$ and $\bar{C}_4$ are good to only five and three significant figures, respectively, and that even the sign of $\bar{C}_8$ is in doubt. Many more figures are reported in Table 9 because the Hessian matrix for the least squares fit has a low eigenvalue implying that there exist many, nearly equally good, sets of parameters but for any one of these sets the individual parameter values should be compatible with one another. All ΔE_L values

Table 9. Dimensionless parameters in the 8-parameter continued fraction, Eq. (172), determined by weighted least squares fitting to 176 accurately computed values of ΔE_L with $L > 24$. Values of C_1 and $\bar{C}_2$ are held fixed and the remaining six parameters are allowed to vary freely

	$\bar{C}_k$
2	0.7884289062
3	0.256090151
4	3.09784765
5	−48.4079555
6	87.515153
7	42.52027
8	−12.1991

with $L \leqslant 200$ are known to at least 16 significant figures. The 176 ΔE_L's with $L \geqslant 25$ are fitted to at least nine significant figures using the parameters reported in Table 9, but the fit is rather insensitive to the values of $\bar{C}_k$ with $k > 5$. The ΔE_L with $L < 25$ are discarded because they are overly sensitive to $\bar{C}_k$ with $k > 8$. The resulting continued fraction is smooth for all L, i.e. when the truncated continued fraction is recast in the form of a Padé approximation, both polynomials (in numerator and denominator) have no positive zeroes. We do not find a practical application of the continued fraction formula (172), but we do find it reassuring that (168) has a well behaved logical extension.

Hill's analysis strongly suggests that the value of the dimensionless $\bar{C}_2$ parameter is related to the physical size of the electron cloud. Let us rewrite (169) in terms of the average radius, $\tilde{r}$, (expressed in atomic units) of a normalized radial distribution function, $\tilde{p}(r)$:

$$\bar{C}_2 = 1 - 2\tilde{r}/(5\pi), \tag{173}$$

$$\tilde{r} = \int_0^\infty r\,\tilde{p}(r)\,\mathrm{d}r, \tag{174}$$

$$= 15\sqrt{\pi}/16 \quad \text{for Kais function.} \tag{175}$$

Straightforward manipulation of Hill's equations relates $\tilde{p}(r)$ to $\Psi(1, 1)$ for any ^1S two-electron wave function, $\Psi(1, 2)$:

$$\tilde{p}(r_1) = \tilde{n} r_1^5\, \Psi^2(1, 1), \tag{176}$$

$$= r_1^5 \exp(-r_1^2) \quad \text{for Kais function,} \tag{177}$$

where $\tilde{n}$ is the normalization factor such that $\int_0^\infty \tilde{p}(r)\,\mathrm{d}r = 1$. The radial distribution function $\tilde{p}(r_1)$, which requires knowledge of the two-electron wave function, is distinct from the usual radial distribution function, $p(r)$, which requires knowledge only of the electron density [61]. Figure 7 displays plots of $p(r)$ and $\tilde{p}(r_1)$ for the Kais function, given by Eqs. (46) and (177), respectively. Both radial distribution functions peak at roughly the same point and have similar first moments:

$$\int_0^\infty r\,\tilde{p}(r)\,\mathrm{d}r = 1.6617 \text{ Bohr}, \tag{178}$$

$$\int_0^\infty r\,p(r)\,\mathrm{d}r = 1.7445 \text{ Bohr}. \tag{179}$$

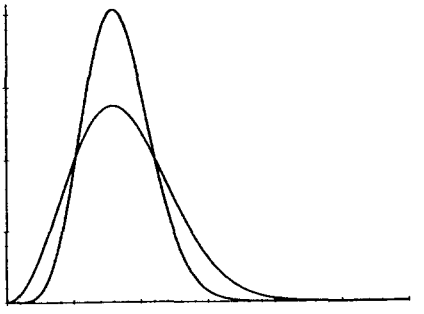

Fig. 7. Comparison of the traditional radial distribution function computed from the one-electron density, with that computed from $\Psi(1, 1)$, the two-electron wave function evaluated when both electrons occupy the same spatial position. The traditional distribution is broader with lower peak height. Both distribution functions are computed for the Kais function and normalized to unity

Table 10. Average radius of the effective radial distribution function, $\tilde{\rho}(r)$, defined in terms of $\Psi(1, 1)$, corresponding value of the $\bar{C}_2$ parameter in the limiting law, and values of closely related parameters in Hill's equation. Atomic units

System	$\tilde{r}$	$\bar{C}_2$	Hill C_1	Hill C_2
Kais function	1.661675	0.788429	0.0167293	0.01061834
Helium atom	0.819755	0.895626	0.0247419	0.00774727
Small limit	0.0	1.0		

It is reasonable to assume that both distributions respond in roughly the same way to changes in parameters in the Hamiltonian that control the size of the electron cloud. For example, it is expected that both distributions contract when the spring constant in the HLM Hamiltonian is increased, or when the nuclear charge of a two-electron ion is increased. The value of $\bar{C}_2$ for the helium atom is expected to be greater than that for the Kais function but less than unity, the limiting value for an infinitely compact charge distribution. This expectation is confirmed in Table 10. Helium atom values reported in the table were obtained by integrating the 230 term wave function of Freund et al. [25, 59, 60].

The second modified version (171) of Hill's two-term asymptotic expansion can be rationalized by pointing out the ubiquitous occurrence of inverse powers of $(\ell + \frac{1}{2})$ in asymptotic expansions of contributions from the ℓth partial wave. Several examples are given above, and more can be found in the literature [11, 33, 32]. Sums of inverse powers of $(L + 1)$ then arise quite naturally when the sum of partial wave contributions is evaluated using the following summation formulas which can be derived using properties of the polygamma function [58]:

$$\sum_{\ell=0}^{L} (\ell + \tfrac{1}{2})^{-4} = \pi^4/6 - (1/3)(L + 1)^{-3} + (4/24)(L + 1)^{-5} - O(L^{-7}), \tag{180}$$

$$\sum_{\ell=0}^{L} (\ell + \tfrac{1}{2})^{-5} = 31\zeta(5) - (1/4)(L + 1)^{-4} + (5/24)(L + 1)^{-6} - O(L^{-8}), \tag{181}$$

$$\sum_{\ell=0}^{L} \left(\ell + \frac{1}{2}\right)^{-6} = \tfrac{1}{15}\pi^6 - (1/5)(L + 1)^{-5} + (6/24)(L + 1)^{-7} - O(L^{-9}). \tag{182}$$

Here $\zeta(k)$ is a Riemann zeta function. The sum in (181) is encountered in evaluating double sums of electron repulsion integrals discussed in Sect. 5.7. Let us carry out a numerical test of (171) for the Kais function. Consider two alternative asymptotic expansions:

$$\Delta E_L = C_1/(L + 1)^3 + C_2/L^4 + C_3/L^5 + C_4/L^6 + O(L^{-7}) \tag{183}$$

$$= C_1/(L + 1)^3 + C_2/(L + 1)^4 + C_3'/(L + 1)^5 + C_4'/(L + 1)^6 + O(L^{-7}). \tag{184}$$

The C_1 and C_2 coefficients are given by Eqs. (48) and (50), respectively. Numerical values of the higher coefficients, determined from (172) and Table 9 are

$$C_3 = -0.050833, \qquad C_4 = 0.16565,$$

$$C'_3 = -0.008360, \qquad C'_4 = 0.10127.$$

Higher-order terms in the improved asymptotic expansion (184) have smaller numerators and larger denominators than those in (183) for our model system. A general proof of this result would appear to be extremely difficult, if not impossible, because these higher-order terms are not fully determined by the correlation cusp. In other words, terms in the Hamiltonian other than the kinetic energy operator and electron-repulsion, r_{12}^{-1}, contribute to the values of C_3' and C_4' and higher coefficients.

5.7 Derivation of the limiting law

The energy error incurred by truncating the partial wave expansion of the Kais function, (159), can be developed as an asymptotic expansion in inverse powers of $(L+1)$ using results of the partial wave analysis. Let us drop all terms of order $O(L^{-5})$ or higher. It follows that we can then drop the normalization factor from (157) since it differs from unity by terms of order $O(L^{-5})$. To show this we write the normalization factor as follows:

$$N_L = \left[1 - \sum_{\ell > L} \langle \Psi^{(\ell)} | \Psi^{(\ell)} \rangle\right]^{-1/2}. \tag{185}$$

Substitute Eqs. (111) and (182) into (185) and collect terms:

$$N_L = 1 + \tfrac{3}{4}C_1(L+1)^{-5} - \tfrac{15}{16}C_1(L+1)^{-7} + O(L^{-9}). \tag{186}$$

The truncation error is the sum of all higher σ_ℓ terms, defined in (165), with a neglible renormalization correction:

$$\Delta E_L = -\sum_{\ell > L} \sigma_\ell + O(L^{-5}), \tag{187}$$

$$\sigma_\ell = T_\ell + V_{\ell,\ell}^{(1)} + 2V_{\ell,0}^{(2)} + \sum_{\ell'=1}^{\ell} (2 - \delta_{\ell,\ell'}) V_{\ell,\ell'}^{(2)}. \tag{188}$$

To expand ΔE_L through terms in $(L+1)^{-4}$ we need σ_ℓ expanded through terms in $(\ell + 1/2)^{-5}$, so we replace T_ℓ in (188) by the first term in (132); we drop $V_{\ell,\ell}^{(1)}$ entirely recalling Eqs. (117) and (111); and we replace $V_{\ell,0}^{(2)}$ by the first term in (150). The only difficult part of the analysis is the evaluation of the finite sum of electron repulsion integrals in (188) leading to the following result to be discussed below, where C_2 is defined by (50):

$$\sum_{\ell'=1}^{\ell} (2 - \delta_{\ell,\ell'}) V_{\ell,\ell'}^{(2)} = \tfrac{15}{4}\sqrt{\pi}C_1(\ell + \tfrac{1}{2})^{-4} - 4C_2(\ell + \tfrac{1}{2})^{-5} + O(\ell^{-6}). \tag{189}$$

Derivation of (189) begins with the evaluation of two finite sums:

$$\sum_{\ell'=1}^{\ell} \frac{2 - \delta_{\ell,\ell'}}{(2\ell' + 3)(2\ell' - 1)} = \frac{2}{3} - \frac{1}{2(\ell + 1/2)} + O(\ell^{-3}), \tag{190}$$

$$\sum_{\ell'=1}^{\ell} \frac{(2 - \delta_{\ell,\ell'})(2(\ell')^2 + 2\ell' + 1)}{(2\ell' + 3)(2\ell' - 1)} = \left(\ell + \frac{1}{2}\right) + \frac{2}{3} - \frac{5}{4(\ell + 1/2)} - O(\ell^{-3}). \tag{191}$$

These summation formulas were generated using the Maple program. The coefficient of $(\ell + \frac{1}{2})^{-4}$ in (189) is obtained by replacing $V^{(2)}_{\ell,\ell'}$ by the first term in (156) and retaining only the first term in (190). That the second term in (156) makes no contribution to the leading term in (189) can be shown using (191). Collect terms in $(\ell + \frac{1}{2})^{-4}$ and compare the resulting leading term in σ_ℓ with that in the kinetic energy formula (132).

$$\sigma_\ell = -3C_1(\ell + \tfrac{1}{2})^{-4} - O(\ell^{-5}) \tag{192}$$

$$= -T_\ell - O(\ell^{-5}). \tag{193}$$

Recall that σ_ℓ is, to within a small renormalization correction, the ℓth energy increment. Equation (193) states that each such individual angular momentum contribution satisfies an *approximate virial relation.* The leading term in σ_ℓ is the sum of a positive kinetic energy contribution and a negative potential energy contribution of twice the magnitude. The ratio of these contributions approaches the value of $-1/2$ in the high-ℓ limit as expected of any situation dominated by inverse-first-power potentials. The HLM Hamiltonian, with its mixture of second-power and inverse-first-power potential energy operators, does not satisfy the usual virial theorem, but it does exhibit the behavior of real-atom Hamiltonians in the sense of (193). The relationship between kinetic and potential energy contributions to σ_ℓ, implied by (193), breaks down for terms in $(\ell + \frac{1}{2})^{-5}$ for the helium atom just as it does for our model system. Inspection of Table 6 reveals large departure from the virial relation when $\ell < 5$. In fact, the leading term in (193) does not even predict the correct algebraic sign of σ_ℓ when $\ell < 2$. Note that kinetic energy makes no contribution at all to the $(\ell + \frac{1}{2})^{-5}$ term which derives entirely from the electron repulsion operator in either the HLM or Helium atom Hamiltonian. See further discussion below. To complete the first step in our derivation of the limiting law, substitute (192) into (187) and evaluate the sum using (180). In this way we recover the leading term in (184) with C_1 coefficient identical to that predicted by Hill's equation (48).

Similarly, the second term in (184) is recovered by summing the second term in (189) using (181). The resulting C_2 coefficient is identical to that predicted by Hill's equation (50). Evaluation of the coefficient of the second term in (189) requires more than a trivial extension of the analysis above. It is obvious from the above discussion that there is no kinetic energy contribution to the second term in (189) and thus to C_2. It is also obvious that various terms all derived from the r_{12}^{-1} operator do contribute. For example, the second term in (190) substituted into the first term in (156) contributes to the second term in (189) as does the first term in (191) substituted into the second term of (156). There are, however, an infinite number of such contributions from higher terms in (156), requiring evaluation of an infinite series. In deriving (156) the $\bar{M}(6, -1, L)$ factors in (151) were expanded in inverse powers of ℓ which is a slowly convergent expansion when $\ell' \approx \ell$. By the same token, the sum over ℓ' in (189) is troublesome. To avoid this problem the summations are reorganized, as briefly outlined below. Substitute (151) into the lhs of (189) to generate a finite double sum over indices ℓ' and ℓ''. Combine the three $\bar{M}$ terms into a single $\bar{M}$ term using (65). Replace the double sum over ℓ' and ℓ'' by a double sum over new summation indices n and m defined as follows assuming ℓ to be an even integer:

$$\ell' = \ell - n, \tag{194}$$

$$\ell'' = 2\ell + n - 2m. \tag{195}$$

Unlike the original sum over ℓ'', the new sum runs over all integers $0 \leqslant n \leqslant m$ and $0 \leqslant m \leqslant \ell$. Expand $\bar{M}(6, -1, L)$ in inverse powers of L and only later make the substitution $L = 2\ell - m$. This expansion is rapidly convergent. Note that m and L are constants in the inner sum over n. The tedious manipulations are performed, of course, by Maple. The result, (189), which has been thoroughly checked numerically, yields one more term in the asymptotic expansion (192):

$$\sigma_\ell = -3C_1(\ell + \tfrac{1}{2})^{-4} - 4C_2(\ell + \tfrac{1}{2})^{-5} + O(\ell^{-6}). \tag{196}$$

The considerable difficulties encountered in evaluating the second term for our simple model system testifies to the heroic analysis of Hill which yields the C_2 coefficient for a general, two-electron, ^{1}S variational wave function.

6 Conclusions

This paper outlines an approach to the electron correlation cusp problem based on the reasonable assumption that by smoothing the correlation cusp one can significantly accelerate the rate of convergence of a CI expansion. Smoothing the wave function is to be achieved by smoothing the singularity in the r_{12}^{-1} electron–electron interaction. Basic to the method are mathematical relationships between extent of smoothing and rate of convergence. This is the first in a series of papers whose goal is a better understanding of the relevant mathematical principles. The subject is studied using a realistic model system for which the exact wave function can be solved in simple closed form. The goals of this first paper in the series are: to establish the credentials of the model by verifying that it correctly reproduces known correlation cusp properties for a Hamiltonian with the traditional r_{12}^{-1} interaction; and to gain deeper insight into how the correlation cusp controls the rate of convergence for that Hamiltonian. Listed below are six conclusions of this study.

(A) The two-electron Hooke's law model provides a simple but meaningful system for testing concepts and methods in the theory of electron correlation. The Kais function provides a remarkably simple but realistic model of dynamic electron correlation, which is the main subject of this paper, but low-lying excited electronic states of the model also provide examples of nondynamic correlation effects to be discussed in future papers. For example, strong mixing of degenerate configurations causes the correlation cusp to disappear entirely in the lowest ^{1}D state. This can be understood in terms of internal angular momentum which keeps electrons apart. Similar internal angular momentum effects are expected to operate in real systems, e.g. the lowest ^{1}D state of the magnesium atom.

(B) The attempt to automate the partial wave analysis of the model using a computer for formal as well as numerical analysis has been a success. Exact formulas for most quantities of interest can be generated recursively starting with one or more of the six representative values of the $M(p, q)$ integral. Convergent continued fraction formulas and asymptotic expansions, useful for formal and numerical analysis of the large-L limit, can also be generated. Many properties of the model can be computed with virtually unlimited numerical precision.

(C) The energy error ΔE_L due to eliminating all functions with angular momentum greater than L from the orbital basis set has been accurately computed for the Kais function. There is no significant difference between the L-dependence of ΔE_L computed for a non-variational, truncated, partial wave expansion and that

computed variationally. In keeping with the results of all earlier studies dating back to the 1962 perturbation-theoretic analysis of Charles Schwartz, ΔE_L is of order $O(L^{-3})$ in the limit of high L.

(D) Hill, in his 1985 analysis of convergence of a variational calculation, developed an asymptotic formula for ΔE_L(FCI) for a two-electron ^{1}S system and showed that the coefficients of the two leading terms in this asymptotic formula can be expressed as integrals over the exact wave function. We show that the energy error due to truncating the partial wave expansion of the Kais function satisfies Hill's equation exactly through terms of order $O(L^{-4})$. Hill's asymptotic equation is recast to avoid the singularity at $L = 0$. This provides a better estimate of ΔE_L for the Kais wave function for all L, and a significantly better estimate for low L. The simplest improved formula is $\Delta E_L \approx C_1(L + \bar{C}_2)^{-3}$ where $\bar{C}_2$ is a dimensionless parameter weakly dependent on the physical size of the atomic system.

(E) Kinetic and potential energy contributions associated with each individual angular momentum subspace in the orbital basis are related approximately by the virial theorem, with the ratio of these contributions approaching $-1/2$ in the high-ℓ limit.

(F) This study concurs with all earlier work in attributing slow $O(L^{-3})$ convergence to difficulties inherent in orbital descriptions of the correlation cusp. This analysis provides what is likely to be the most detailed and numerically precise documentation of this conclusion, and so establishes the model as one which provides a stringent test of ideas to be presented in subsequent papers in this series.

Acknowledgements. This work was supported in part by grant CHE-9108022 from the National Science Foundation. The author thanks Mr. Raymond Roskwitalski, Dr. Andrew Komornicki, and particularly, Professor Werner Kutzelnigg for helpful discussions.

References

1. A theorem by Kato implies that all wave functions in nonrelativistic molecular quantum mechanics are continuous. References in the present paper to "discontinuities" refer to discontinuities in a first, or higher, partial derivative
2. Kato T (1957) Commun Pure Appl Math 10:151. Theorem I establishes the continuity of wave functions. Theorem II establishes nuclear and correlation cusp conditions
3. Hylleraas EA (1964) Adv Quantum Chem 1:1. This article by one of the pioneers in the subject reviews early computations of the helium atom wave function
4. Pluvinage PH (1950) Ann Phys 10:147
5. Roothaan CCJ, Weiss AW (1960) Rev Mod Phys 32:194
6. Bingel WA (1963) Z Naturforschung 18a:1249
7. Pack RT, Byers-Brown W (1966) J Chem Phys 45:556; Carlsson AE, Ashcroft NW, (1982) Phys Rev B 25:3474
8. Kutzelnigg W, Morgan JD III (1992) J Chem Phys 96:4484
9. Rassolov VA, Chipman DM (1996) J Chem Phys 104:9908
10. A very similar symmetry argument, attributed to John D. Morgan III, appears in Appendix E of Ref. [11]
11. Hill RN (1985) J Chem Phys 83:1173
12. Andersson K, Fülscher MP, Karlström G, Lindh R, Malmqvist P-Aa, Olsen J, Roos BO, Sadlej AJ, Blomberg MRA, Siegbahn PEM, Kellö V, Noga J, Urban M, Widmark P-O (1994) MOLCAS, version 3, University of Lund, Sweden

13. Wolinski K, Pulay P (1989) J Chem Phys 90:3647
14. Malrieu JP, Heully JL, Zaitsevskii A (1995) Theor Chim Acta 90:187. This paper presents an overview and comparison of MRPT methods
15. Roos BO, Andersson K, Fülscher MP, Malmqvist P-Aa, Serrando-Andrés L, Perloot K, Merchán M (1996) Adv Chem Phys 93:219
16. White RJ, Stillinger FH (1971) Phys Rev A 3:1521
17. Bartlett JH (1937) Phys Rev 51:661. This paper contains what appears to be the first suggestion in the literature of a logarithmic singularity at the origin in the ground state helium atom wave function
18. Fock VA (1954) Izvestiya Akademii Nauk USSR Ser Fiz 18:161; Engl. translation: D Kngl Norske Videnskab Selsk Forh (1958) 31:138, 145
19. Frankowski K, Pekeris C (1966) Phys Rev 146:46; 150:366; Frankowski K (1967) Phys Rev 160:1
20. Morgan JD III (1986) Theor Chim Acta 69:181
21. Baker JD, Freund DE, Hill RN, Morgan JD III (1990) Phys Rev A 41:1247
22. Engels B (1994) J Chem Phys 100:1380
23. Bartlett JH, Gibbons J, Dunn C (1935) Phys Rev 47:679. This early analysis was subsequently strengthened as summarized in footnote 1 in Ref. [20]
24. Kinoshita T (1957) Phys Rev 105:1490; 115:366; Koga T, Morishita S (1995) Z Physik D 34:71; Koga T (1996) J Chem Phys 104:6308
25. Freund DE, Huxtable BD, Morgan JD III (1984) Phys Rev A 29:980. Results for the 476-term trial function are reported in Ref. [21] p. 1254
26. Umrigar CJ, Gonze X (1994) Phys Rev A 50:3827
27. Klahn B, Bingel WA (1977) Theor Chim Acta 44:9, 27. This paper presents a readable discussion of convergence criteria with chemically meaningful examples of the inadequacy of completeness-in-the-mean-type convergence in the sense of a Hilbert space L^2 norm. Klahn and Bingel prove stronger completeness in what some other authors call the second Sobelev space
28. Thakkar AJ, Koga T (1994) Phys Rev A 50:954
29. Pekeris CL (1958) Phys Rev 112:1649
30. Kais S, Herschbach DR, Levine RD (1989) J Chem Phys 91:7791
31. Char BW, Geddes KO, Gonnet GH, Leong BL, Monagan MB, Watt SM (1991) Maple V Language reference manual, Springer, New York; Char BW, Geddes KO, Gonnet GH, Leong BL, Monagan MB, Watt SM (1992) First Leaves: A tutorial introduction to Maple V, Springer, New York; Blachman NR, Mossinghoff MJ (1994) Maple V quick reference, Brooks/Cole Publishing, New York
32. Schwartz C (1962) Phys Rev 126:1015, (1963) Methods Comp Phys 2:241
33. Klahn B, Morgan JD III (1984) J Chem Phys 81:410
34. Carroll DP, Silverstone HJ, Metzger RM (1979) J Chem Phys 71:4142
35. Schmidt HM, v. Hirschhausen H (1983) Phys Rev A 28:3179
36. Decleva P, Lisini A, Venuti M (1995) Int J Quantum Chem 56:27
37. Bukowski R, Jeziorski B, Rybak S, Szalewicz K (1995) J Chem Phys 102:888; Kutzelnigg W, Klopper W (1991) J Chem Phys 94:1985; 94:2020; Termath V, Klopper W, Kutzelnigg W (1991) J Chem Phys 94:2002; Klopper W, Almlöf J (1993) J Chem Phys 99:5167; Klopper W (1995) J Chem Phys 102:6168; Noga J, Tunega D, Klopper W, Kutzelnigg W (1995) J Chem Phys 103:309; Klopper W, Schütz M, Lüthi HP, Leutwyler (1995) J Chem Phys 103:1085; Schütz M, Klopper W, Lüthi HP, Leutwyler (1995) J Chem Phys 103:6114; Klopper W, Noga J (1995) J Chem Phys 103:6127; Persson BJ, Taylor PR J Chem Phys, in press
38. Kestner NR, Sinanoğlu O (1962) Phys Rev 128:2687
39. Tuan DF (1969) J Chem Phys 50:2740; White RJ, Byers-Brown W (1970) J Chem Phys 53:3869; Benson JM, Byers-Brown W (1970) J Chem Phys 53:3880
40. Kellman ME, Herrick DR (1980) Phys Rev A 22:1536; Krause JL, Berry RS (1985) Phys Rev A 31:3502; Berry RS, Krause JL (1986) Phys Rev A 33:2865
41. Kais S, Herschbach DR, Handy NC, Murray CW, Laming GJ (1993) J Chem Phys 99:417
42. Laufer PM, Krieger JB (1986) Phys Rev A 33:1480
43. Filippi C, Umrigar CJ, Taut M (1994) J Chem Phys 100:1290
44. Taut M (1993) Phys Rev A 48:3561

45. Eddington AS (1946) Fundamental theory, Cambridge Univ. Press, Cambridge; Coleman AJ (1967) Int J Quant Chem Symp 1:457
46. There are also internal and external principal quantum numbers, but we are not concerned with them
47. Press WH, Flannery BP, Teukolsky SA, Vetterling WT (1986) Numerical recipes, Cambridge Univ Press, Chap 16
48. Kutzelnigg W, Morgan JD III (1996) Z Physik D, in press
49. Moore CE (1971) Atomic energy levels, NBS Circular 467 Volume I, US Government Printing Office, Washington, DC, p. 107
50. Hill defines C_1 to be the integral in Eq. (47). We define it by Eq. (48). We conjecture that wherever C_1 appears in this paper it would be given by Eq. (47) if the Kais function were replaced by any other two-electron ^{1}S eigenfunction of a Hamiltonian with any of a broad class of one-electron, central-field potentials. We make no claim to have proved this conjecture, although Hill's analysis constitutes a partial proof. Of course we do claim that wherever C_1 appears in this paper it is given by Eq. (47) in the special case of the Kais function
51. Edmonds AR (1960) Angular momentum in quantum mechanics. Princeton Univ. Press, Princeton See Eqs. (3.7.17) and (4.6.4)
52. For a closely related treatment see pp. 1187–1188 and Appendix E in Hill's 1985 paper [11].
53. Abramowitz M, Stegun IA (1964) Handbook of mathematical functions, NBS Applied Mathematics Series 55, US Gov. Printing Office, Washington, DC. We adopt the notation of Abramowitz and Stegun unless explicitly stated otherwise in the text
54. The continued fraction formulas (83)–(85) are apparently new, but closely related to a formula attributed to Wallis. See Eq. (6.1.49) in Ref. [53]
55. Perkins, JF (1968) J Chem Phys 48; 1985. Perkins reports expansions of r_{12}^k for integral values of $k \geqslant -1$
56. Piero Decleva, private communication. Contrary to what is stated in the captions to Figs. 4–11 in Ref. [36], the quantites plotted there are partial wave amplitudes multiplied by factors of $r_1 r_2$
57. All numerical and nonnumerical computations for this paper were carried out on a small work station, either a Sun/4 with 16 Mbytes of memory or a Silicon Graphics Indy with 32 Mbytes
58. Polygamma functions are discussed in Sects. 6.4 and 6.8 in Ref. [53]. For a useful asymptotic expansion in terms of Bernoulli numbers, see Eq. (6.4.11) and Table 23.2
59. See pp. 1182–1183 in Hill's 1985 paper [11]
60. An alternative estimate of the Hill coefficients for the helium atom is $C_1 = -a/3 = 0.0247170$ and $C_2 = -b/4 = 0.00791400$ where a and b, obtained by fitting variationally computed energy increments, are reported on p. 36 in Ref. [36]. These estimates agree well with the more accurate values reported in Table 10 taken from Ref. [11]
61. Alternatively one could define $\Psi^2(1, 1)$ to be a modified, nonnormalized, density function. Then Hill's C_1 and C_2 coefficients are proportional to the third and fourth moments, respectively, of the corresponding radial distribution function